3. THE DESIGN OF THE UP-CSIR BALSS

Although not precisely in the scope of this thesis, the design of the bioreactor and BALSS circulation system underlie some of the studies presented below. For the sake of illustration it is therefore useful to provide information in this regard. However, in view of proprietary issues this is unfortunately only generically possible.

Broadly speaking, both the bioreactor and circulation system have progressed through two design iterations and are in the process of a third. The system design engineer was Mr. AJ van Wyk of the department of Mechanical Engineering of the University of Pretoria [110,111].

3.1 Bioreactor optimization

As part of a Mechanical Engineering project [112] Mr. LJT Ronné of the Department of Mechanical engineering employed particle tracking computational flow dynamics (CFD) to optimize the bioreactor for even flow and mass transport throughout the open-cell polyurethane foam (PUF) cell aggregation matrix in the bioreactor. The attractive biocompatibility characteristics of this matrix resulted in its choice in this case. The PUF had a mean cell volume of approximately 1 mm diameter allowing the formation of large hepatocyte aggregates (this is investigated in section 4.2.3).

The radial flow geometry of the bioreactor (figure 3.1) was chosen to perfuse a maximal possible PUF volume (and thus aggregated cells). However, following both *in vitro* and *in vivo* experiments it became apparent that the overall first-iteration bioreactor shape had areas of flow stagnation, i.e. ‘dead’ spaces, where hypoxic circumstances would inevitably result. CFD modeling of this bioreactor then confirmed what had been observed in practice (figure 3.2)

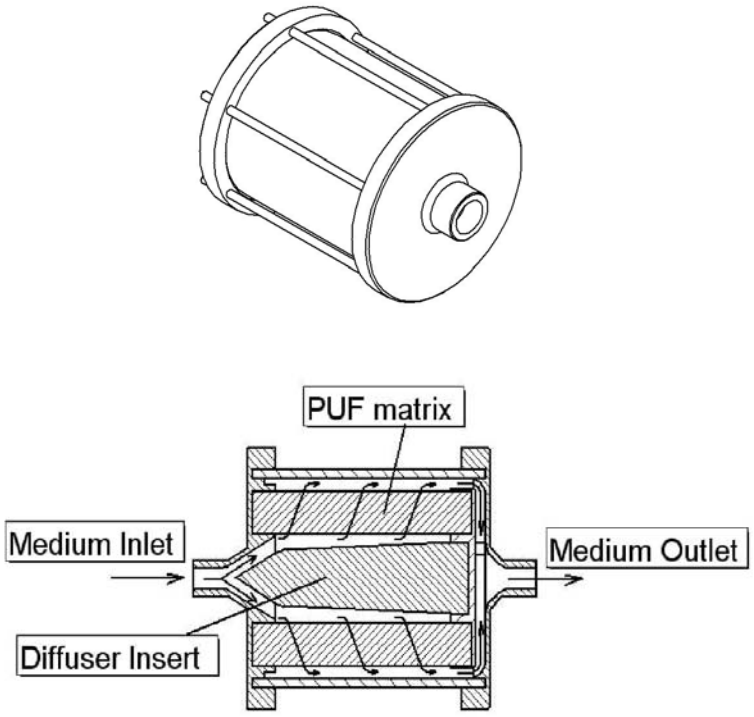

Figure 3.1 First iteration, non-flow optimized bioreactor

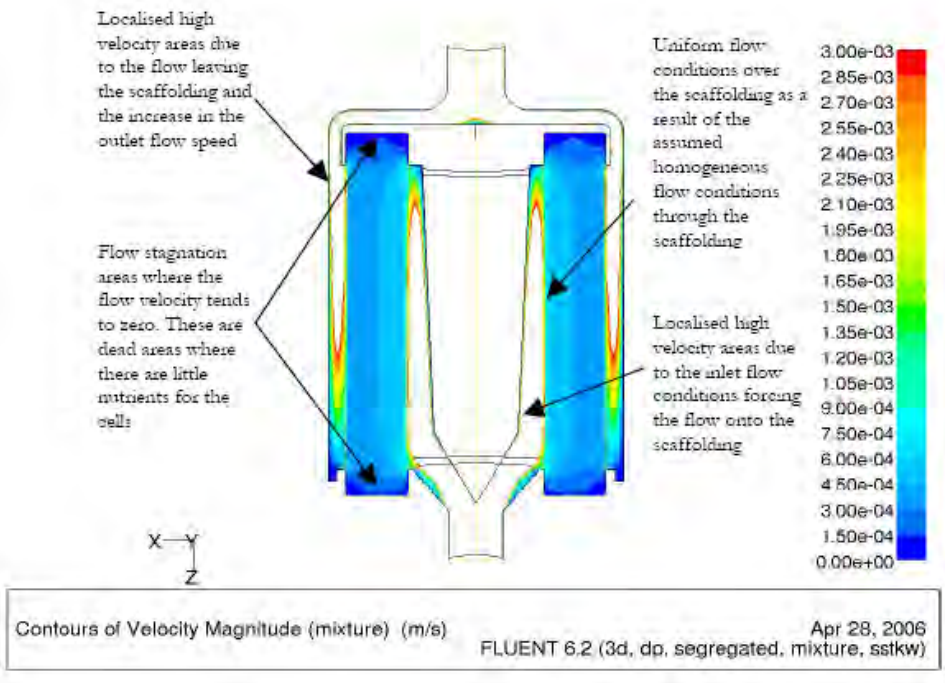

Figure 3.2 CFD model of velocity contours of a plasma-PFC mixture over the PUF cell aggregation matrix in the non-optimized bioreactor configuration (this figure was reprinted with permission of Mr. LJT Ronné [112]).

In response to these problems the bioreactor design was then changed to ensure that the plasma-PFC mixture would perfuse all of the PUF matrix evenly, with no 'dead spaces', ensuring that all aggregated cells received the same oxygenation and mass transfer conditions. To make this possible the bioreactor was basically shortened on the long axis and the foam support was redesigned.

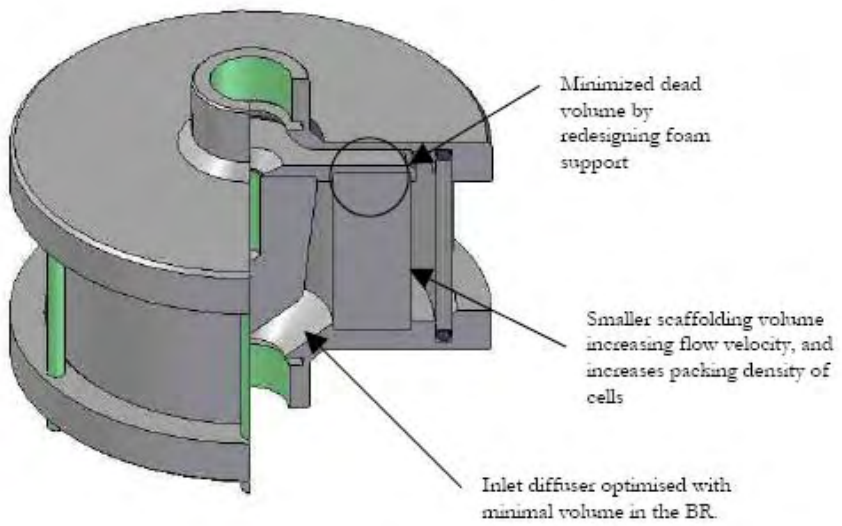

Figure 3.3 Optimized bioreactor design. The dead spaces have all been removed.

As before, the redesigned bioreactor was then simulated using CFD and it was confirmed that there was homogenous flow throughout the matrix (figure 3.4). Having said this, the internal configuration and material composition of the bioreactor, including the aggregation matrix, are currently being reviewed. A third, presumably considerably better, iteration will hopefully result.

As a matter of interest, the first iteration bioreactor was used in the first of the bioreactor-*in vitro* studies (section 4.2) and in the evaluation of the UP-CSIR BALSS in a large animal model (section 5.3). Thereafter, the optimized bioreactor was employed in the second bioreactor-*in vitro* study (section 4.3).

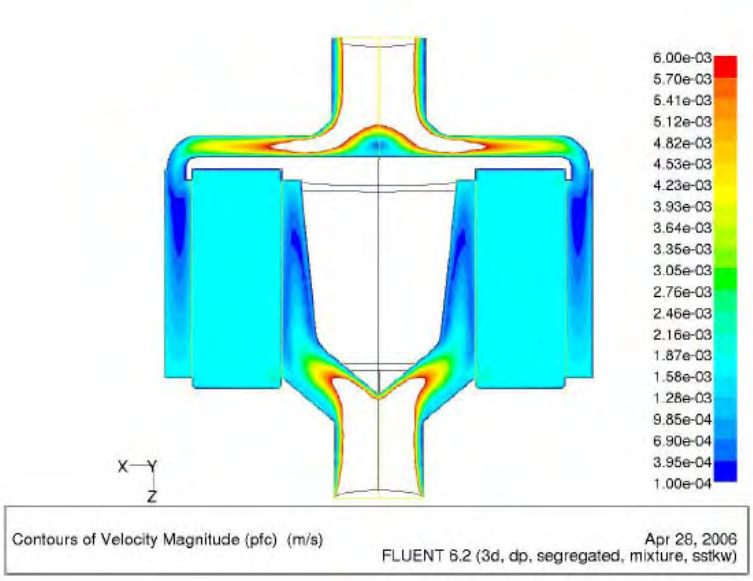

Figure 3.4 CFD model of velocity contours of the plasma-PFC mixture over the PUF cell aggregation matrix in the optimized bioreactor configuration. The removal of 'dead' areas was confirmed (reprinted with permission of Mr. LJT Ronné [112]).

3.2 BALSS circulation system optimization

The design of the BALSS circulation system (figure 3.5) incorporates the following components:

- An intravenous (IV) blood input line, normally from the jugular vein, which proceeds to,
- A plasma separator, as is routinely used in dialysis applications, enabling the input of plasma-only at 70-100 ml/min into the system. The separated cellular component of the blood is passively returned to the patient.
- A reservoir, into which the plasma flows and is mixed with a 40 % v/v PFC emulsion, doubling its volume so that the resulting PFC concentration is 20 % v/v. The resulting PFC-plasma mixture then flows through,
- An in-circuit neonatal oxygenator, fed with an external gas supply, which oxygenates the mixture, followed by,
- A bioreactor as described above, which is perfused with the plasma-PFC mixture. The cells therefore treat oxygen-rich plasma, facilitating their synthetic and toxin clearance functions. The internal bioreactor circulation system circulates more rapidly than the plasma inflow rate in order to further improve mass transfer functions. Thereafter,

- A PFC filter then separates the PFC from the 'treated' plasma, which rejoins the cellular component of the initially separated blood and returns to the patient. The separated PFC, on the other hand, returns to the abovementioned reservoir where it is re-mixed with the incoming plasma as already described.

The specifications of the filters, some sub-circulation flow rates, gas supply and the details regarding control and monitoring are aspects of the proprietary 'know-how' of the system and are therefore not listed.

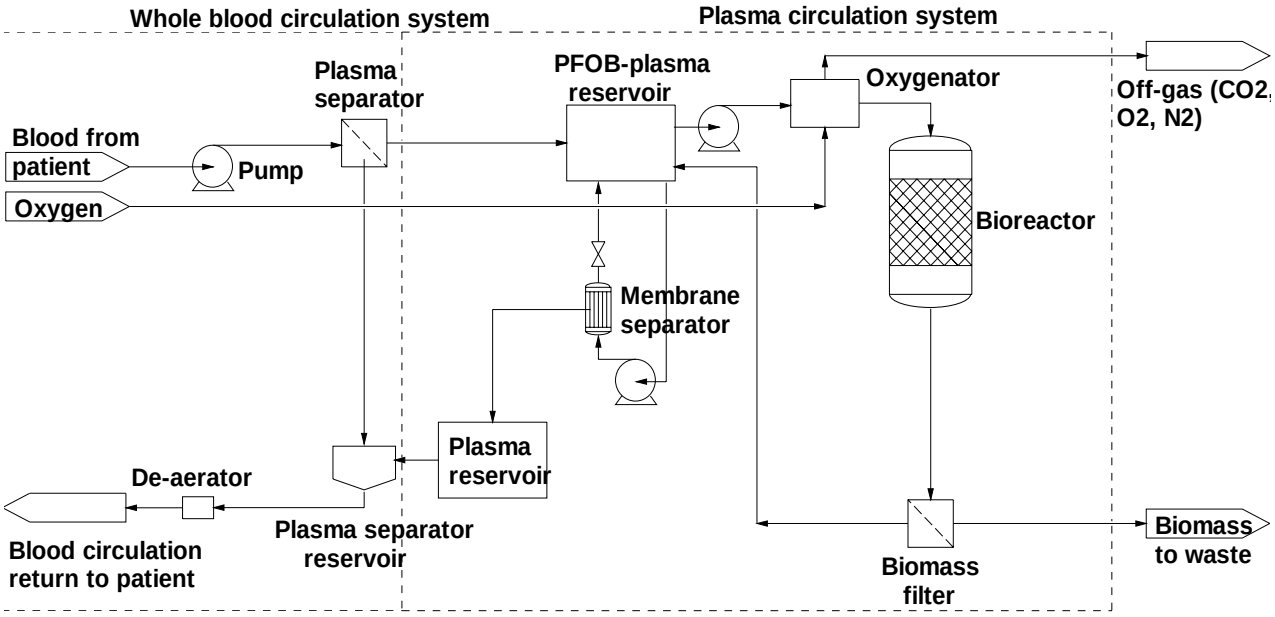

Figure 3.5 Schematic of the UP-CSIR BALSS (reprinted with permission from Mr. K van Wyk, system designer).

The first of the circulation system iterations (the mark I model, figure 3.6) was designed prior to the accumulation of empirical data regarding the behaviour of the system. The system was, visibly, rather complex and used tubing and components normally used in laboratories rather than in the clinical environment.

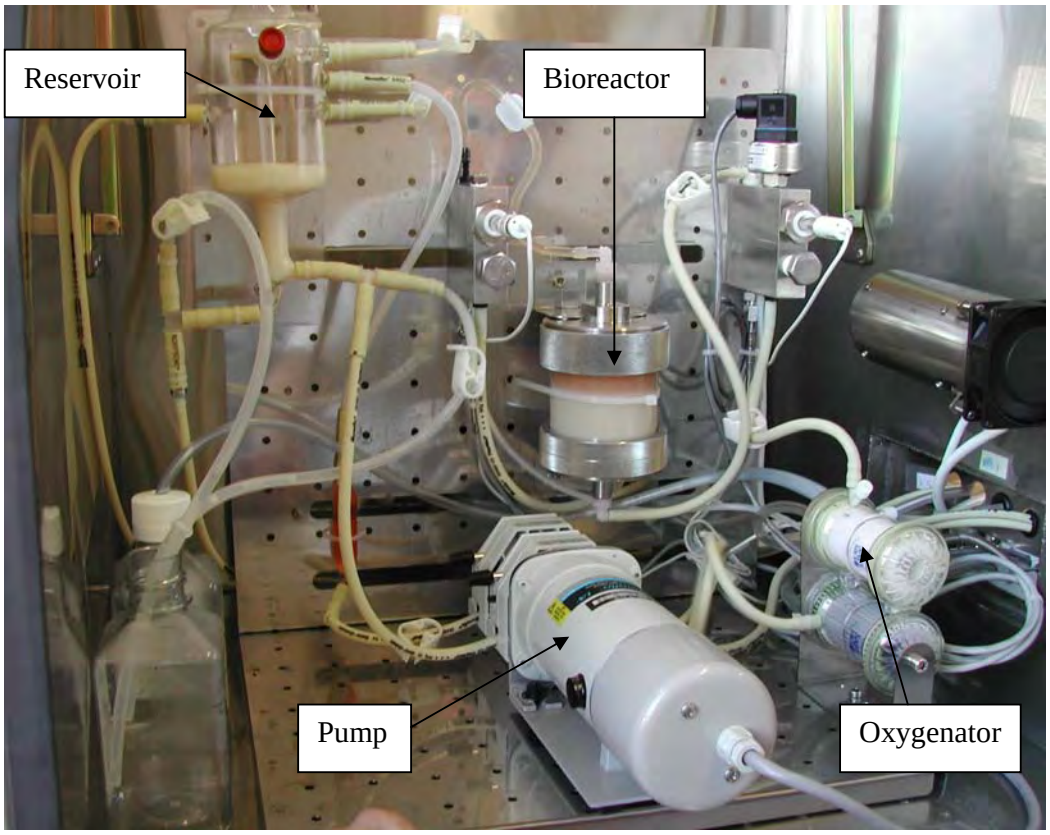

Figure 3.6 The BALSS mark I system. The components were more appropriate to a laboratory than clinical setting.

However, the mark I system was useful for collecting design parameter data in 5 animals. This led to a complete redesign, resulting in the mark II (figure 3.7) which was optimized for subsequent clinical evaluation in large animals (section 5.3.1 below). The mark II, although identical in principle to the mark I, employed as far as possible, tubing and components normally used in the clinical setting. However, the mark II was still understood to be a research device: It contained sensors for flow, pressure and temperature, blood gas and even biochemistry (section 6.3.4) which enabled *on-line* system monitoring and data collection that would be valuable for additional system redesign subsequently. The mark II had a graphical user interface (GUI) enabling the direct control of all system parameters including manual shutdown if necessary. In the event of power outages it was also equipped with a programmable logic controller (PLC) and uninterruptible power supply (UPS), so that system functions would not terminate even following the potential loss of access to the GUI.

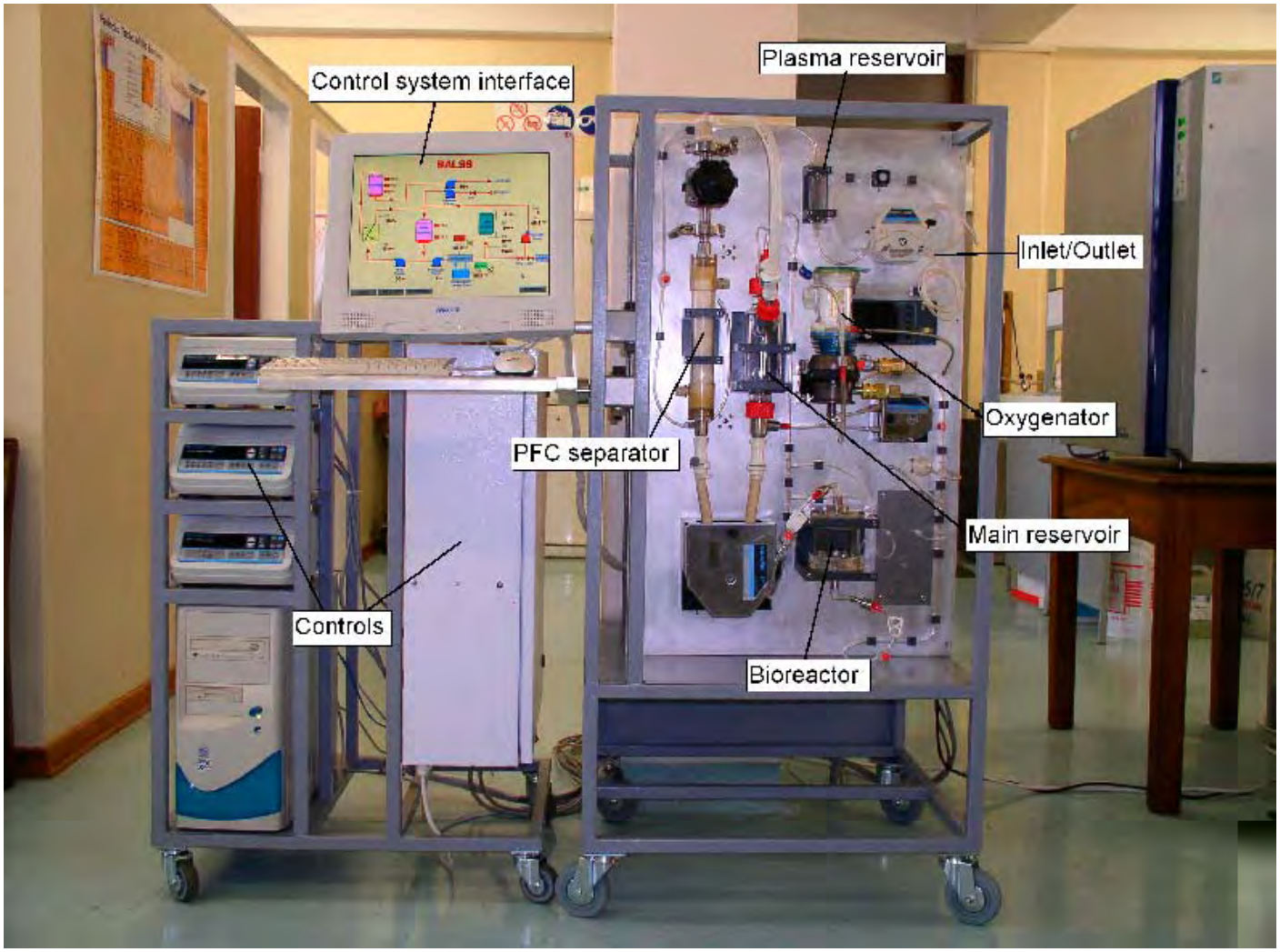

Figure 3.7 Annotated image of the UP-CSIR mark II BALSS

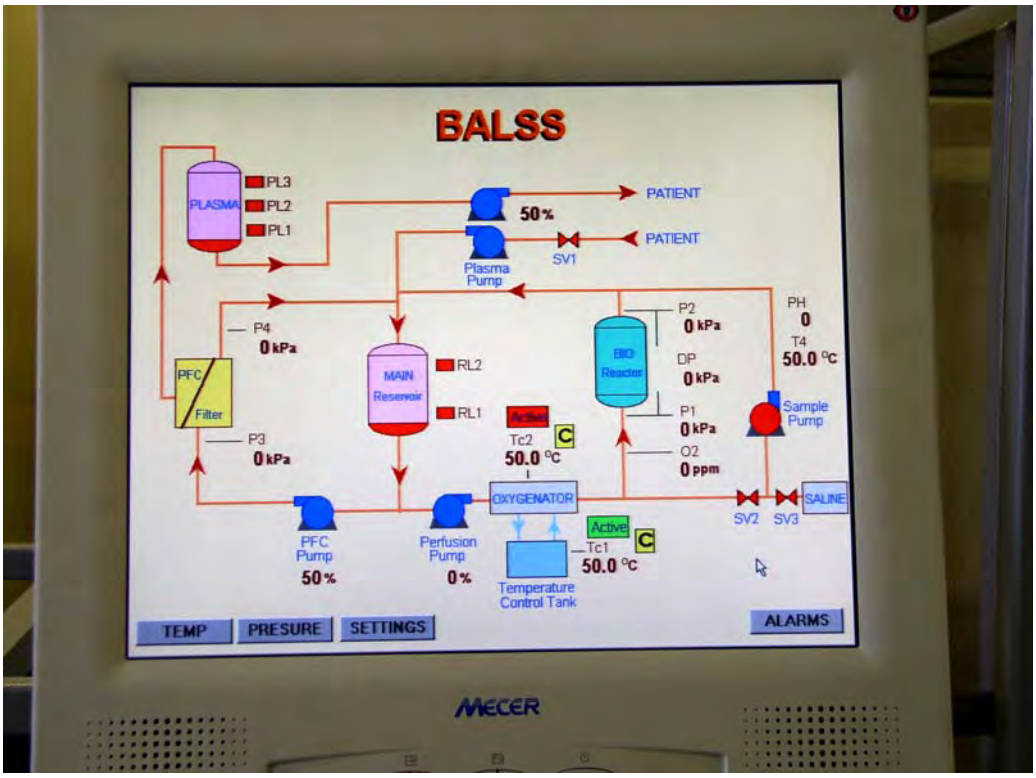

Figure 3.8 Graphical user control interface for the mark II model. Direct control was possible for the system as a whole and all sub-circulation flow rates.

During large animal trials (section 5.2 below) a comprehensive intensive care unit (ICU) was assembled and in which the mark II BALSS was evaluated for clinical efficacy in animals (figures 3.9,10). Simutaneously, a large amount of data was collected regarding the operation of the system itself. Particularly the following became apparent regarding the mark II:

- It was bulky, i.e. required a large amount of space.
- It required excessive attention to the sterile preparation of some of the components prior to treatment, which consequently took long.
- Particular components were not GMP/FDA approved.
- It was complex and required skilled personnel to control it during treatments.
- Its 'behaviour' changed over the course of treatments as a result of coagulation effects in the system.
- Some of the materials used in the system could have been improved for biocompatibility, e.g. the use of steel and glass in the first iteration bioreactor.
- The extracorporeal volume was greater than 1 litre, i.e. rather large, which may have contributed to haemodynamic instability in some of the patients.

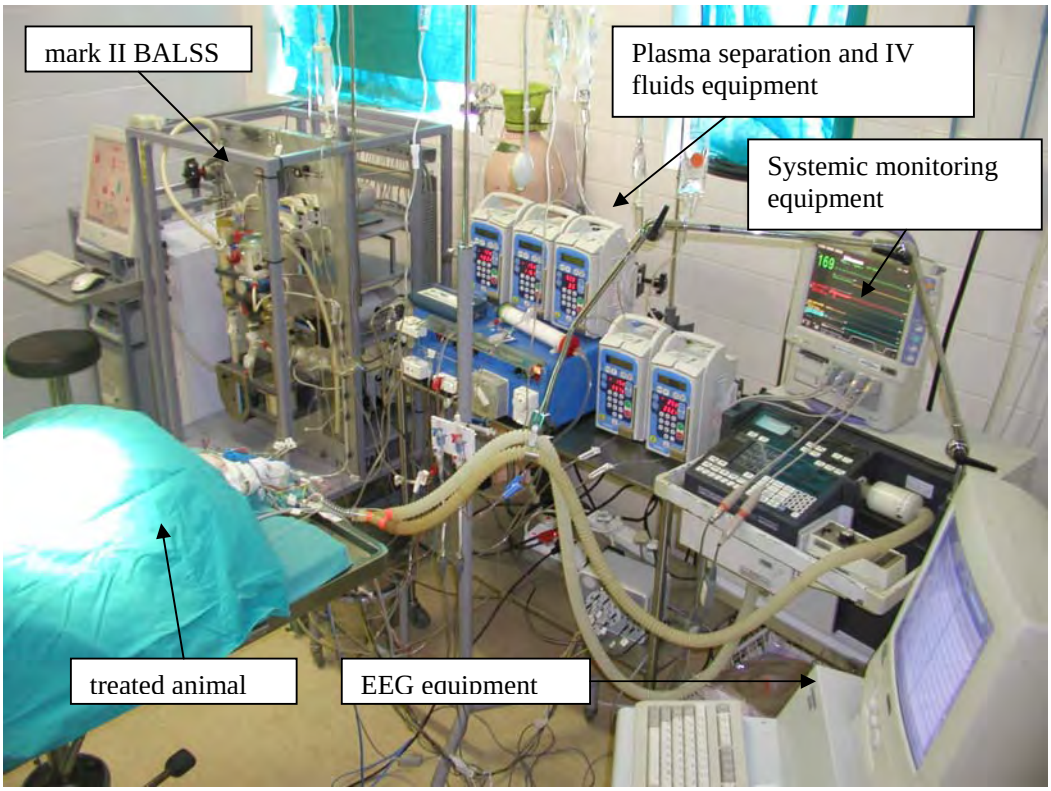

Figure 3.9 Intensive care unit (ICU) in the evaluation of the mark II BALSS.

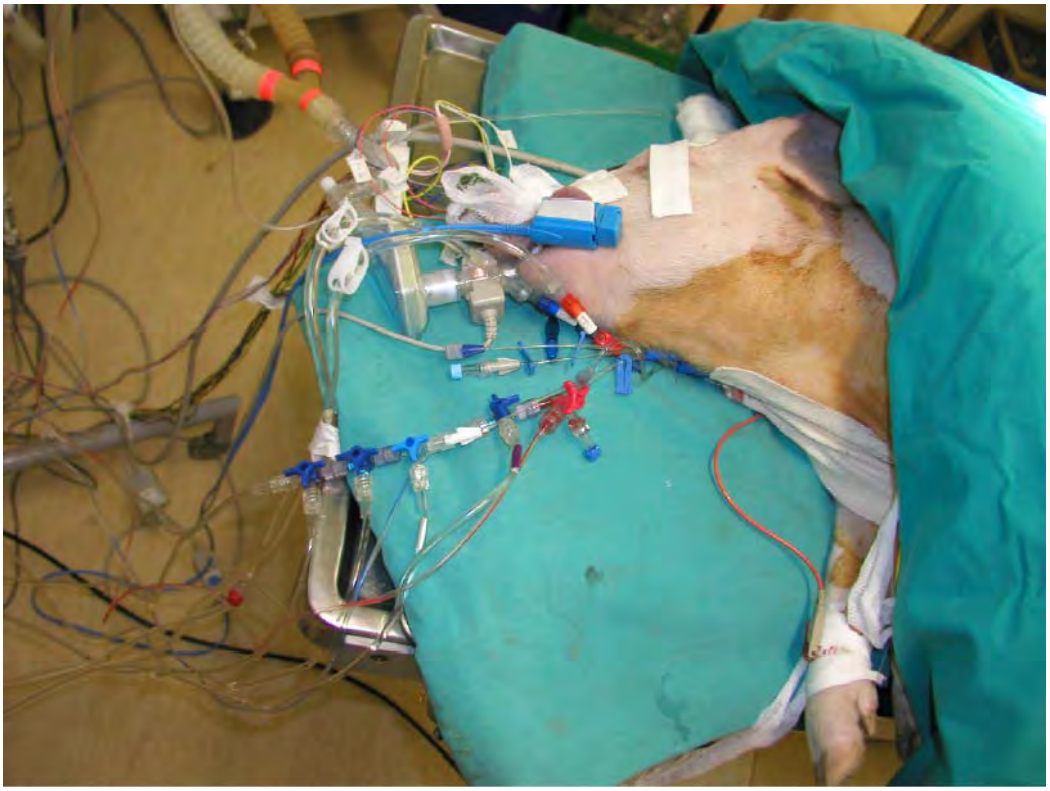

Figure 3.10 Animal undergoing a BALSS treatment. The blood lines configuration was complex.

These findings led to a comprehensive review of the required improvements. These may be summarized as follows:

- The use of more biocompatible materials in all parts of the system with emphasis on preventing coagulation effects.
- Bioreactor and oxygenator redesign.
- Extensive *in silico* system modeling for operational parameter optimization.
- A decrease in the overall size of the system to a bed-side unit.
- A decrease in the internal volume of the system.
- Attention to the ergonomics and aesthetics of the device.
- The operational simplification of the system so that a dialysis technician with minimal training would be able to operate it.
- The compilation of all standard operating procedures, i.e. a system manual.
- The use of, as far as possible, pre-sterilized standard dialysis equipment.
- GMP/FDA approval for all materials, suppliers and operating procedures.

Based on an examination of the history of institutions conducting similar work, these findings and/or requirements are generic for all BAL's. Following the implementation of the above, a mark III version will result, and its purpose will be to conduct additional animal experiments before proceeding to safety and efficacy trials in humans. It is expected that the mark III will be the final version in the design-optimization-redesign cycle that has been underway.

4. *IN VITRO* CELL BIOLOGY STUDIES

Overview

The following section presents three studies in which *in vitro*, biologically-based models of the BAL system have been developed. These models are designed to demonstrate or enable the metabolic functionality of the bioreactor component of the BAL and are *scaled-down* or simplified laboratory versions of the system. The studies are presented in a logically progressive order as determined by the methods or findings consecutively established.

The first of the studies details a sterile method for isolating large quantities of primary cells (hepatocytes), the metabolically active component of a BAL bioreactor of this type. Without cells in requisite quantities, such bioreactors would be insufficiently functional to fulfill the intended clinical need. Thus, such methods (or models) are a formal necessity for BAL systems. In this case the success of the method is evaluated in terms of impacts on cell functionality and the quantities isolated. Comparisons are made with previously published methods and the particular benefits of this one are highlighted.

The second study investigates the metabolic activity of cell-seeded bioreactors in a scaled-down recirculation system (model) of the BAL. This aims to demonstrate the metabolic function of the bioreactors as determined by their design, including the novel application of a perfluorocarbon (PFC) oxygen carrier, relative to controls. A variety of issues determining the relative success of these demonstrations (and thus of the model) are discussed. For example, design and methodological differences between studies, the effect of cell density on bioreactor metabolism and the impact of the oxygenating gas mix concentration when using PFC.

The third study similarly aims to demonstrate bioreactor metabolic functionality while employing PFC in a model version of the BAL, but differs in terms of improvements in the employed methods following knowledge evolution in the field. Specifically, the simultaneous use of radio-transparent small-scale bioreactors with and without PFC, seeding with co-cultures rather than hepatocyte-only monocultures, alteration of the gas mixes to more physiological O_2 levels and the novel use of positron emission tomography for studying primary cell bioreactor metabolism on the same time-scale as would occur in the treatment of a patient with a BAL.

Thereafter, thoughts and recommendations follow regarding alternate potential cell sources that may meet all the requirements of the global BAL device regulatory authorities. As was stated, a sterile large-scale cell source (model) is a formal necessity for the development of an effective BAL device. Examples mentioned include the development of genetically engineered swine and human chimeric animals. The problems surrounding presently existing transformed and primary cell sources are also discussed to provide additional clarity to the above arguments.

4.1 A large scale automated method for hepatocyte isolation: effects on proliferation in culture

Nieuwoudt MJ, Kreft E, Olivier B, Malfeld S, Vosloo J, Stegman F, Kunneke R, Van Wyk AJ, Van de Merwe SW.

Cell Transplantation 2005; 14(5): 291-299.

4.1.1 Introduction

Efficient, non labour-intensive and sterile methods for isolating large quantities of hepatocytes are desirable in the development of artificial liver support systems for the treatment of acute liver failure (ALF) [113]. There is some debate regarding exactly how many cells are required in order to adequately fulfill the needs of treating an adult human being in ALF [83]. However, considering cost and practicality, an increased hepatocyte yield in each procedure is a highly desirable end point. Porcine livers and hepatocytes are useful for establishing isolation methods since they have anatomical and physiological similarities to human livers and hepatocytes and have unlimited availability [114].

The purpose of this study was to evaluate a novel numerically high-yield hepatocyte isolation method as compared to the traditional centrifuge method. We investigated the impact of the isolation procedures on the hepatocytes for 7 days during subsequent in vitro culturing, using trypan blue counting, flow cytometry, phase-contrast microscopy, the lactate to pyruvate ratio, LD and AST leakage, albumin production and lidocaine clearance.

4.1.2 Materials and Methods

Media and Chemicals

All media and chemicals are as defined by Nieuwoudt *et al* [87] and presented in Appendix A.1.

Animals, liver preparation and perfusion

Non-fasted pathogen-free, female, white Landrace pigs of 20 kg average mass were prepared for surgery by intramuscular injection of 0.75mg/kg midazolam (Dormikum, Roche) and 10mg/kg of ketamine (Anaket, Centaur). After intubation, anesthesia was maintained by continuous infusion of propofol (Diprivan, Astra Zeneca) at 2.5 mg/kg/hr with ventilation using medical oxygen.

Briefly, a midline incision was made from xiphisternum to pubis. The portal vein was dissected out to the level of the pancreas and the small pancreatic branches were clamped and divided. Two ligatures were placed around the portal vein and between a small incision was made into which the bubble-end of a size 4.0 (5.6 O.D.) endotracheal (ET) tube was inserted to the level of the bifurcation of the vein. The ET tube was secured into place and gravitational perfusion commenced using 1L of supplemented clinical saline, followed by 1L of University of Wisconsin (UW) solution. After hepatectomy, the liver was placed in a sterile polypropylene dish and gently massaged until complete blanching could be observed, and then transported to the in vitro laboratory.

Upon arrival, the polypropylene dish was placed on a raised grill inside a stainless steel dish that was housed in a laminar flow cabinet. The ET tube was connected to a circulation loop (LS25 Masterflex tubing, Swiss Labs Johannesburg SA), which accessed the various buffers (figure 4.1.1). A Masterflex peristaltic pump was used to circulate the buffers through the liver. Initially 1L of the perfusion buffer containing EDTA was used (Buffer 1), followed by 2L without EDTA (Buffer 2) and then the waste outlet was clamped, enabling recirculation of the collagenase solution at 30 ml/min until the liver became jelly-like in consistency. After 5 recirculations the liver capsule would normally rupture, whereupon flow was terminated and the liver combed to a cellular mass using a broad-toothed steel comb. The same initial procedure was used in either isolation method; thus, the hepatocyte yield per liver was expected to be similar.

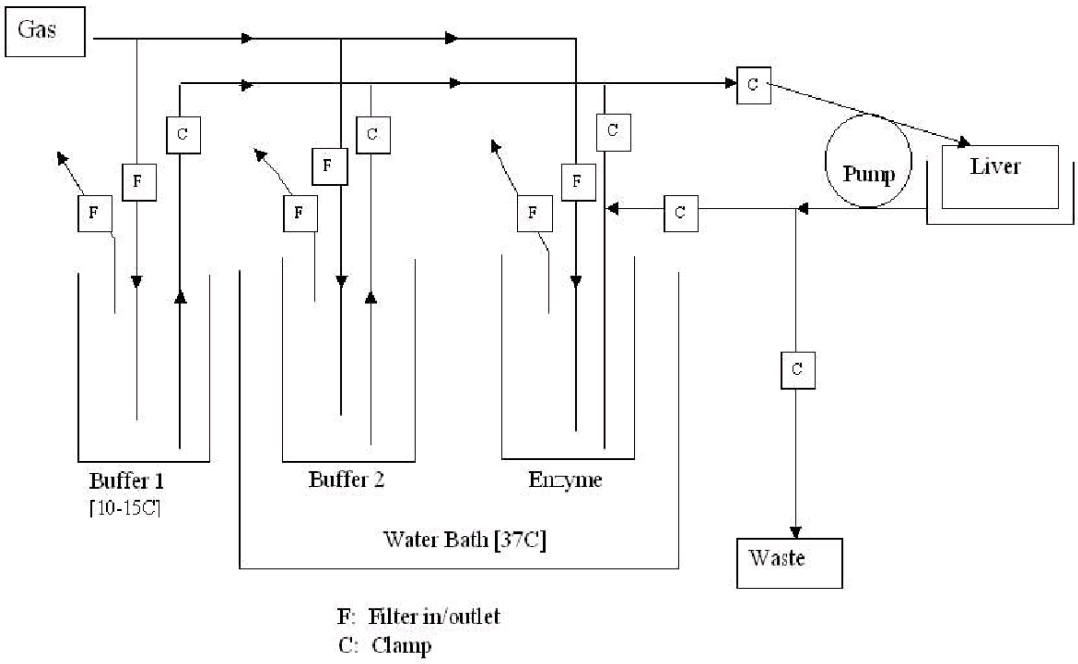

Figure 4.1.1 Schematic of Perfusion Apparatus

Hepatocyte isolation procedures

Using modified minimum essential culture medium (MEM) the cell suspension was washed from the dish into a 250µm nylon mesh that was folded into a filtration funnel. The funnel was mounted on a glass flask that was designed to enable either vacuum filtration or oxygenation (figure 4.1.2). To the vacuum inlet was connected a Sartonet pump, while the oxygenation inlet was clamped, allowing vacuum filtration of the suspension into the flask. During filtration the suspension in the filter was massaged using the round end of a 100ml sterile test tube, while MEM was added as needed. After the initial filtration, the filtrate was agitated then transferred to a 100-µm filter in the funnel of another flask and filtration again followed. Two different isolation procedures were then compared. In the first procedure all of the cell filtrate was decanted into 50 ml centrifuge tubes, normally 12, and a 'manual' isolation protocol was followed as is described below in A. In the second procedure, B, the Baylor Rapid Autologous Transfusion (BRAT) machine was employed in addition to two samples upon which the centrifuge method, A, was employed in parallel.

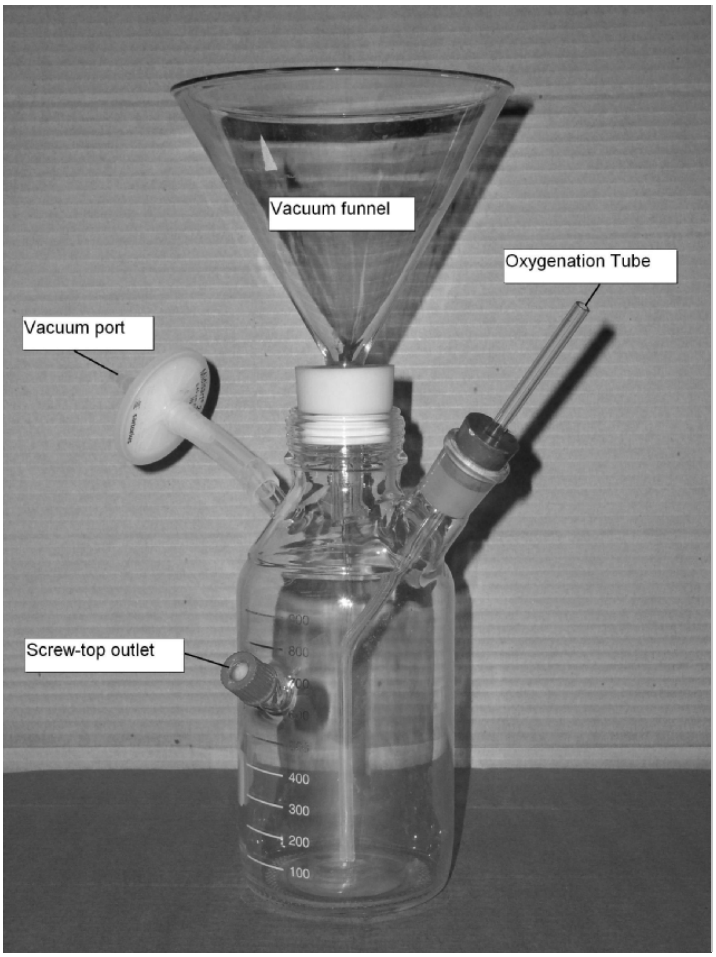

Figure 4.1.2 Oxygenation flask

Procedure A: 40 ml samples of the agitated cell filtrate were poured from the screw-top outlet of the oxygenation flask and used to perform a 'manual' hepatocyte isolation procedure, which in principle is the traditional method described by several authors [115-117]. Briefly, the suspension was centrifuged at 40G for 5 minutes at 4 ^{o}C, then washed with MEM and centrifuged 3 times at 30G for 4 minutes at 4 ^{o}C. Percoll:HBSS solution, as described in Appendix A1 (Percoll solution), was mixed with the cell pellet to achieve a concentration of 1.06 g/ml, that is, 11 ml of the Percoll solution with 20 ml of the cell-pellet suspension in each of the 50 ml tubes. Centrifugation followed for 10 minutes at 50G. Following separation of the hepatocytes from the non-parenchymal cells, 3 MEM washing steps followed for 4 minutes each at 30G. A hepatocyte-only suspension then remained.

Procedure B: While gently oxygenating the cellular filtrate in the oxygenation flask, containers with 2L of Wash buffer, 1L of supplemented MEM and 300 ml of Percoll solution were placed in the laminar flow cabinet. A BRAT machine was placed adjacent to the cabinet (figure 4.1.3]. In essence, the function of this machine is to transfer cells through sterile tubing by means of a peristaltic pump to a centrifuge, where centrifugation achieves cell separation based on density. The apparatus is composed, respectively, of a fixed volume transparent centrifuge bowl (either 250 ml or 165 ml) that clamps into the centrifuge housing, connected to a length of subdivided plastic tubing that is fitted into the peristaltic pump, allowing the alternate filling or emptying of the bowl in the directions of waste, washing or filling solutions (figures 4.1.4,5). The centrifuge bowl (figure 4.1.5) is designed to spin on a rotating ceramic joint, and is composed of an inner and outer wall allowing the cleaning and separation of cell fractions by allowing fluid entry into the bowl during centrifugation.

In these procedures the centrifuge speed was manually set to 50G, in the hardware, and used at that speed throughout the procedure. Using the filling line, cell suspension was sucked out of the oxygenation flask into the centrifuge bowl. Since the volume of the cell suspension was always larger than that of the bowl, to transfer the entire cell suspension required several fill cycles and these were done without stopping the centrifuge. To clean cell debris from the cell suspension after each 3-minute centrifugation cycle, wash buffer was passed down the washing line at the peristaltic pump’s lowest speed, 200 ml/min, until the waste line became clear. After each cycle, to provide the cells in the bowl with a physiologically preferable medium, the wash buffer in the bowl was displaced with oxygenated, supplemented MEM and the cells were allowed to resuspend by stopping the peristaltic pump.

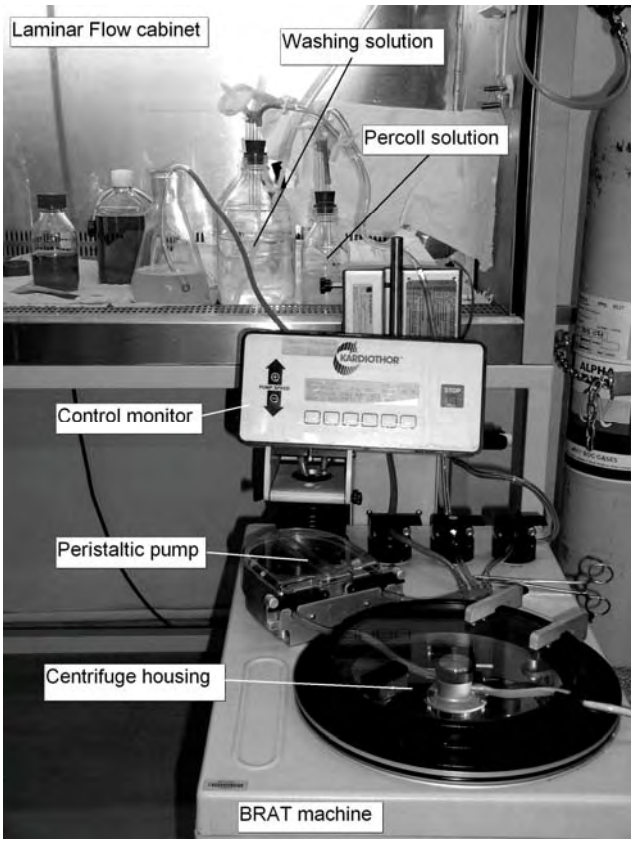

Figure 4.1.3 The BRAT machine

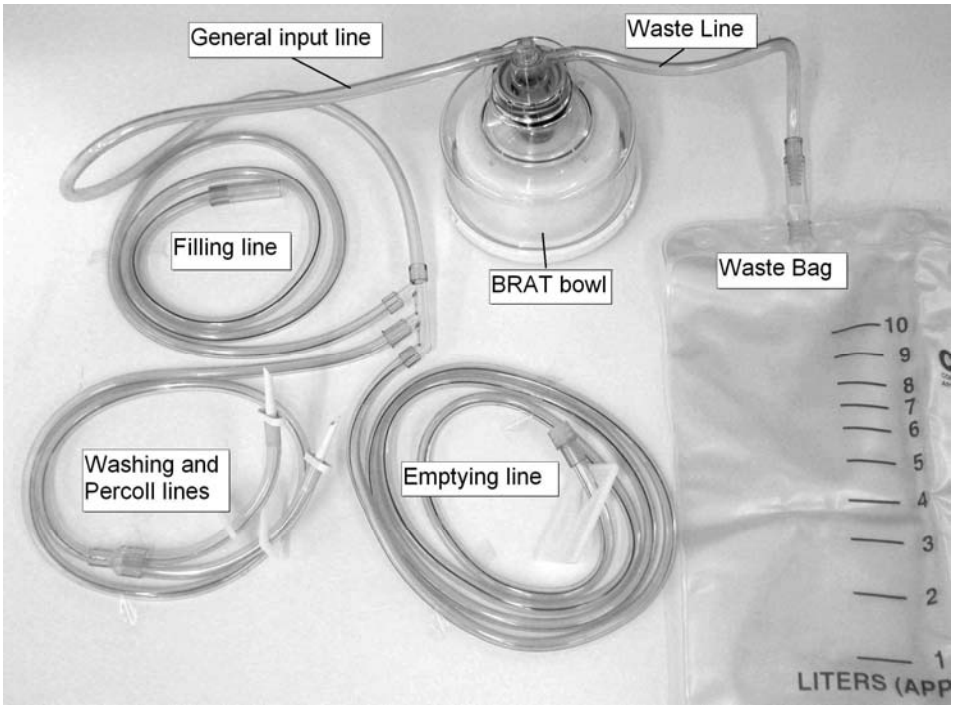

Figure 4.1.4 Disposable BRAT apparatus

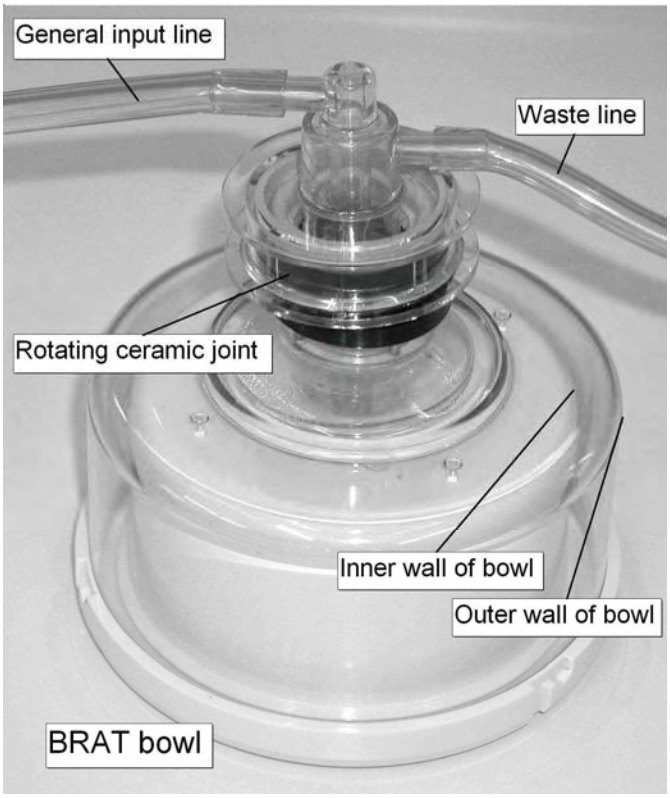

Figure 4.1.5 BRAT bowl

To create a density gradient between the non-parenchymal and hepatocyte cell fractions, the MEM remaining in the bowl after the last cycle was displaced with Percoll solution, followed by centrifugation at 50G for 10 minutes. The volume of the Percoll solution added depended on the volume of the bowl, 137.5 ml for a 250ml bowl and 90.8ml for a 165ml bowl. However, a great benefit of this method is that the addition of Percoll could be terminated during centrifugation, when it was observable that a clear separation had formed between the parenchymal and non-parenchymal cell fractions in the bowl. This is possible since the two cell fractions are different in colour (figures 4.1.6a, 6b) and it was confirmed by comparing the two fractions under light microscopy subsequently. The non-parenchymal cell supernatant was then removed from the hepatocyte fraction using 4 wash buffer-MEM cycles. A hepatocyte-only suspension then remained and it was pumped out of the bowl through the emptying-line into a second oxygenation flask. The final volume of the suspension was noted for hepatocyte yield and viability calculations.

Figure 4.1.6a BRAT Bowl prior to addition of Percoll. Separation has not yet occurred.

Figure 4.1.6b BRAT Bowl after addition of Percoll. Separation has occurred.

Hepatocyte culturing and evaluation methods

All employed methods are as described by Nieuwoudt et al [87] and also presented in Appendix A.2.

Briefly, cell suspensions from the Centrifuge and BRAT procedures were evaluated for viability and cell count. Flow cytometry was conducted on cells immediately after the procedures to determine the effects of oxygenation, and also on cells in 2D culture flasks to determine the impact on the cell cycle 3 and 7 days after seeding. The resulting DNA histograms indicated the relative cell cycle status of the suspension, that is, the proportion of DNA in the G0/G1, S or G2M phases. Daily media sampling evaluated hepatocyte viability by means of LD and AST leakage and to examine the state of cellular oxidation and aerobic metabolism by means of the lactate to pyruvate ratio. On day 2 galactose elimination, on day 3 urea production, on day 4 lidocaine clearance and on day 5 albumin production was measured. Digital micrographs, were taken at day 3 and day 7 after seeding to examine if cell populations were proliferating normally and to confirm the sterility of the procedures.

All values are presented as the mean $\pm$ the standard deviation. Where appropriate P values ($P<0.05$) were calculated using the 2-tailed Mann-Whitney t-test to indicate significant differences.

4.1.3 Results

Isolation procedures

Table 4.1.1 presents cell yield and viabilities produced by the Centrifuge and BRAT procedures. In agreement with Morsiani *et al* (1995) [118], our finding was that two to three people are able to perform the centrifuge procedure in 40-45 minutes. With the BRAT machine one person could perform the procedure in 20-30 minutes. As was expected, the hepatocyte yield per liver was comparable in that the same initial procedure was used. However, differences in hepatocyte viability were apparent: With the centrifuge procedure, viability was 92.5 % $\pm$ 1.29, while with the BRAT procedure, viability was 95.91 % $\pm$ 2.95. The deceased viability of cells from the

centrifuge method was possibly due to cell damage caused by increased contact with plastic centrifuge vials, and an increase in the duration of the isolation procedure. The success of an isolation procedure was determined by media aliquots testing pathogen free.

Table 4.1.1 Yield and viability of hepatocytes per liver, following isolation using Centrifuge and BRAT technology

Mass of pigs	Sample Size	Hepatocyte Yield (Centrifuge)	Hepatocyte Yield (BRAT)	Cell viability % (Centrifuge)	Cell viability % (BRAT)
Mean = 20.1 kg	Centrifuge = 6	Mean = 5.2 $\pm$ 2.1 x 10^9	For **250ml bowls** Mean = 7.3 $\pm$ 5.37 x 10^9	Mean = 92.5 $\pm$ 1.29	Mean = 95.91 $\pm$ 2.95
	BRAT 250 ml = 8 165 ml = 6		For **165ml bowls** Mean = 2.8 $\pm$ 1.0 x 10^9		

Note: *Values are represented as means $\pm$ standard deviation.

The vacuum filtration/oxygenation flask (figure 4.1.2) was found to be very efficient in aiding cell filtration. However, oxygenation prior to and during the BRAT procedures was found to facilitate hepatocyte aggregation, in so doing, hindering accurate cell counting. This observation is in agreement with the findings of previous authors [119-121]. Since it is difficult to accurately count cells when there are clumps present, cell counts are represented in table 4.1.1 as counts excluding aggregates. Thus, the values are minimal amounts relative to those actually present. To decrease aggregation, either manual or magnetic stirring was employed and this was partially successful.

Microscopy

Daily microscopic observation of hepatocyte cultures revealed no discernable differences between cells that originated in either procedure. Both procedures resulted in cytoplasmic vacuolization and granularities that steadily decreased and normally disappeared by the fourth day after seeding. It was observable that all viable cells had attached prior to the first change of culture medium 12 hours after the isolation procedures and no cell debris was visible in the discarded medium every 24 hours

thereafter. During the first 4-5 days the attached hepatocytes grew cytoplasmic extensions and cell spreading was the predominant process. By the 7-th day the culture was usually nearing confluence, although the Flow cytometry results indicated that the cells were still dividing (figure 4.1.8). Digital micrographs taken at day 3 indicated that vacuoles were present in addition to cytoplasmic extensions. By day 7, all granularities and vacuolization had disappeared.

Flow Cytometry.

A comparison of hepatocyte DNA profiles following oxygenation or not during the BRAT procedure (figure 4.1.7) revealed that the G_0/G_1 phase was dramatically increased when oxygenation had not taken place, 74.18%, as opposed to when it had, 40.04%. In addition, the S and G_2M phases were increased when oxygenation had occurred as opposed to when it had not, that is, BRAT + O_2, S = 46.15% and G_2M = 13.82%, while BRAT – O_2, S = 22.36% and G_2M = 3.46%. This result suggests that lack of oxygenation caused G_0/G_1 cell cycle arrest, whilst oxygenation promoted cell cycle progression. However, the benefit must be weighed against the fact that hepatocyte aggregation is also facilitated by oxygenation. Nonetheless, this was an interesting observation that will benefit from further study.

After 7 days following the BRAT procedure 37.59% of the DNA was in the S phase, as opposed to 32.02% at 3 days, while with the Manual procedure at 7 days, 34.57% of the DNA was in the S phase, as opposed to 27.62% at 3 days. Two tailed, Mann-Whitney tests ($P<0.05$) revealed no significant differences when the G_0G_1, S and G_2M phases at Day 3 were compared in the two procedures, while the same was found at Day 7. Additionally, no statistically significant differences were observed when Day 3 was compared to Day 7 (figure 4.1.8). This indicated that cell harvesting using the BRAT system had no negative impacts on cell replication, relative to the Manual method.

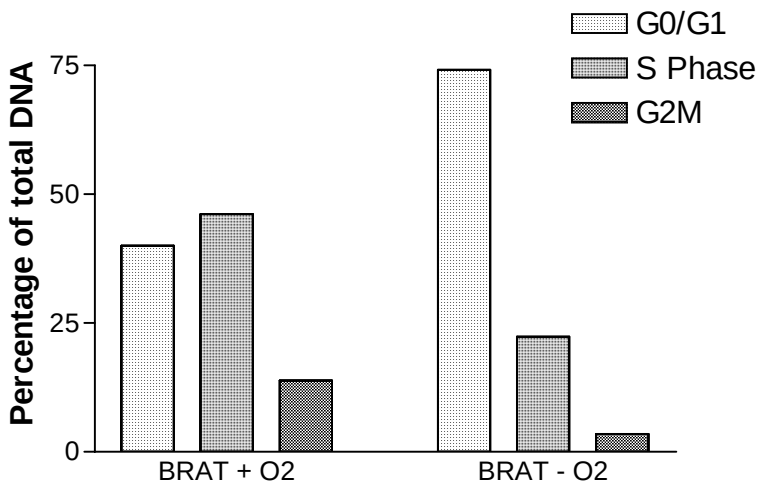

Figure 4.1.7 Flow Cytometry: DNA profile after BRAT procedure with and without oxygenation and prior to culturing

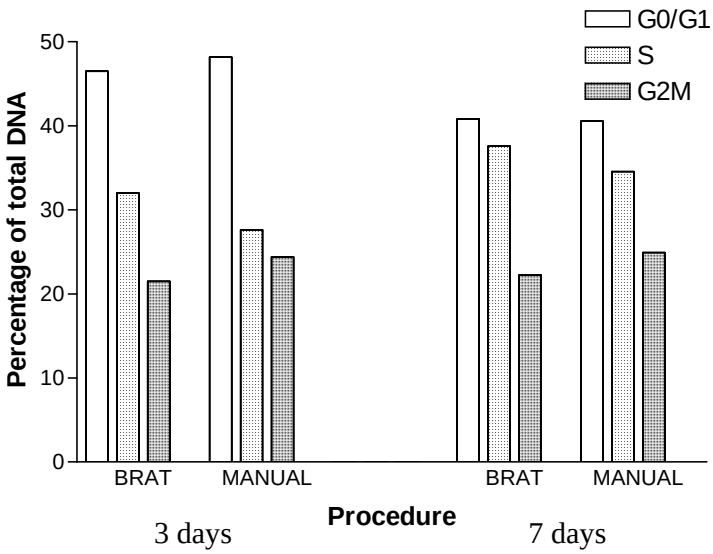

Figure 4.1.8 Flow Cytometry: DNA profile after 3 and 7 days culturing

Biochemical Analyses

In agreement with the microscopic and flow cytometry findings, no significant differences could be determined between the Centrifuge and BRAT methods. The trend was for the lactate to pyruvate ratio to decline towards day 3 after isolation and

then to stabilize for the remainder of the isolation period. The decline in the ratio was due almost entirely to a change in the lactate concentration. LD and AST similarly decreased and stabilized after 3-4 days in culture, indicating a progressive stabilization of the culture towards Day 7. Lidocaine clearance was measurable and found to be a mean of 7.37 ± 4.7 µg/hr/Million cells in experiments conducted at Day 4 after isolation. This result indicates that the cytochrome P450 system was active at that stage. At Day 5, albumin production could be measured and averaged 14.76 ± 0.61 µg/hr/Million cells.

4.1.4 Discussion

The development of effective cell-based bio-artificial liver assist devices relies on the isolation of large quantities of hepatocytes. In this study we describe a largely automated and sterile hepatocyte isolation procedure wherein high cell yield and viability were achieved following surgical removal of the liver. Attention to the composition and utilization of each perfusion step undoubtedly improved cell survival and viability. The centrifuge based isolation method using the modified Seglen protocol is well described [113,115-117]. However, this method is time consuming, which may negatively impact hepatocyte viability. In addition, it is limiting in terms of hepatocyte isolation from large animals since multiple handling steps may decrease viability, as was observable in the results, while increasing the likelihood of bacterial contamination. It should also be noted that while establishing *in vitro* laboratory isolation procedures, repetition is required in order to develop skills. Since only the results of successful experiments are presented, the development of these skills is not apparent. Thus, using a procedure that minimizes potentially un-sterile handling is of obvious benefit.

By using the BRAT machine, isolated cells could be handled in a manner that was guaranteed to be sterile. The historical application of this device was in the cleaning of whole blood products. An advantage of this method is that it is possible to control the addition of the Percoll solution during centrifugation, based on observing the separation of hepatocytes from non-parenchymal cells. Morsiani *et al* (1995)[118], have previously described a high yield isolation procedure using a COBE 2991 Cell Processor as opposed to the BRAT machine. A benefit of the BRAT machine is that,

similar to the COBE 2991, the disposable tubing and centrifugation apparatus is sealed and sterile. The differences between the machines are, firstly, the COBE 2991 uses a flexible donut-shaped bag, while the BRAT uses an inflexible fixed volume bowl, and secondly, while the former has added functionality, the latter is considerably less expensive. In addition, prior to the centrifugation steps we used a novel filtration/oxygenation flask as opposed to an orbitally shaken filtration apparatus: We found vacuum filtration of the post-enzymatic cell suspensions to be very efficient. Advantages of both the oxygenation/filtration flask and the BRAT procedure are that it is possible to oxygenate the cell-suspensions and media during the procedure. The results of flow cytometry suggested that oxygenation facilitated cell division, indicating that it was beneficial to proliferation.

As was to be expected, a comparison of cell yields between the two procedures revealed that they were comparable. The benefits of the application of the BRAT machine lie in convenience and speed, the ability to oxygenate during the procedure and guaranteed sterility. Sterility is of critical importance if the bioreactor is to be employed in a clinical application. The use of the BRAT machine did result in high cell yields (7.3×10^9 for 250ml bowls) and viabilities (95.91%) when compared with previous studies (83,113,115,116,118]. Flow cytometry confirmed that the hepatocytes were progressively recovering after the isolation procedures and tended toward proliferation between Days 3 and 7. No significant difference could be detected between cells from the Centrifuge and BRAT procedures and these observations were confirmed by microscopic and biochemical studies. Our general observation was that isolated hepatocytes only regained their functional polarity after 3-4 days in a culture configuration excluding an extracellular matrix and this appears to be in agreement with the findings of previous studies [113,122-124]. This observation obviously has bearing on the timing of the use of prim**a**ry cells in bioartificial liver devices or in *in vitro* drug testing.

In conclusion, we have established a large-scale, automated, sterile and reproducible procedure whereby large quantities of viable porcine hepatocytes may be isolated, using technology normally available in large-centers.

4.2 A study to determine hepatocyte function in the UP-CSIR radial-flow bioreactor using a perfluorocarbon oxygen carrier

Nieuwoudt M, Moolman S, Van Wyk AJ, Kreft E, Olivier B, Laurens JB, Stegman F, Vosloo J, Bond R, van der Merwe SW.

J Artif Org 2005; 29(11): 915-918.

4.2.1 Introduction

The aim of this study was to determine the effect of bioreactor design and the inclusion of a circulating oxygen carrier on the *in vitro* metabolic activity of hepatocytes in a simplified BALSS circuit. The UP-CSIR BALSS [10,94] incorporates a direct hepatocyte-plasma contact, radial-flow bioreactor with a polyurethane foam (PUF) matrix. The open-cell pore size of the PUF matrix is on average 500 µm, each of which may incorporate an aggregate with 15 000 or more hepatocytes. The internal volume of the PUF matrix is 250 ml, thus, a total of 6×10^{10} cells or 300 g may be seeded, accounting for 20 % of a normal liver's hepatocyte mass. This should be sufficient to maintain the estimated minimal requirements for liver support [83,84].

An ongoing concern amongst investigators is the presence of domains of low O_2 tension and hypometabolism in their bioreactors [83,107]. To overcome potential mass transfer limited domains within the UP-CSI bioreactor a perfluorocarbon (PFC) oxygen carrier that is incorporated in the bioreactor sub-circulation has been developed. Perfluoro-octyl bromide (PFOB) is a synthetic perfluorinated aliphatic compound with high gas solubility. It is chemically and biologically inert and tends to be both hydrophobic and lipophobic. Thus, it requires emulsification (normally with lecithin) prior to use in a recirculating aqueous environment [10,94].

This study investigates, using established indicators of liver function, firstly, the metabolic activity of hepatocytes seeded into the PUF matrix of the radial-flow

bioreactor, and secondly, the performance of the bioreactor is compared, with and without PFC, to monocultures.

4.2.2 Materials and methods

All media and chemicals used in the cell culturing, transport and dissolution of the liver are as described by Nieuwoudt *et al* (2005)[87]. Perfluorocarbon-lecithin emulsions were prepared according to the method of Moolman *et al* (2004) [10,94]. The emulsions were mixed with double concentrated MEM and sterile deionised water, to achieve a 20% v/v PFC emulsion-MEM mixture. The mixture was pH adjusted and used as a culturing medium. For liver perfusion and hepatocyte isolation the method of Nieuwoudt *et al* (2005)[87] was used throughout.

Cell count and viability was assessed with Trypan-blue. The suspension was then seeded into a sealed recirculating system in an incubator, representing a simplified *dynamic* model of the BALSS. Briefly, each system (figure 3.2.1) was composed of LS 25 Masterflex tubing that connected a 500 ml glass reservoir, a 100 ml internal volume bioreactor, with a sampling port, and the reservoir medium was oxygenated using an aquarium bubbler. All was housed in a non-gas incubator at 37 ^{o}C (Scientific 2000, Instrulab, South Africa). To facilitate homogenous seeding throughout the matrix, the bioreactor was designed for even flow using computational fluid dynamics (CFD), see section 3 above. A total of eight, 7-day long metabolic trials were conducted on the *dynamic* and *static* systems. Five studies employed ordinary MEM, (PFC(-)), while 3 used the supplemented PFC-MEM emulsion (PFC(+)).

Cell culturing and metabolic evaluation

All methods are as defined by Nieuwoudt et al [88] and presented in Appendix A3.

Briefly, daily samples were taken for LD, AST, glucose, lactate and pyruvate. Blood gas samples for pH, pO_2, pCO_2 were taken and the oxygen uptake rate (OUR) was calculated.

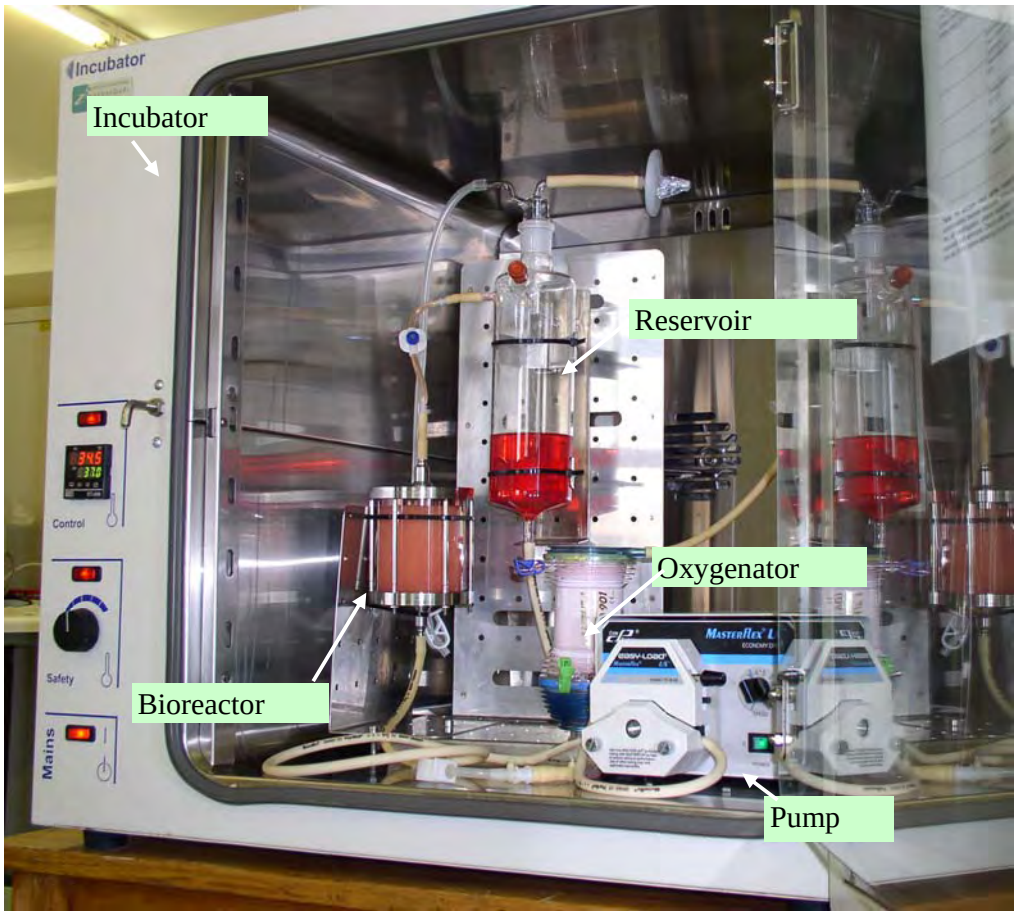

Figure 4.2.1 Simplified *in vitro* dynamic model of the BALSS

Metabolic clearance/production studies were performed in both dynamic and static configurations: on day 2 D(+)galactose elimination, on day 3 ammonia detoxification and urea synthesis, on day 4 lidocaine clearance and on day 5 albumin production. Upon termination on day 7, imaging studies involved either scanning electron microscopy (SEM), to investigate the presence of cells in the foam, or isotopic scanning to examine the seeded-distribution of active hepatocytes in the foam. The latter was performed following the injection of a 300 µCi dose of ^{99m}Tc-labeled-DISIDA N-(2,6-diisopropylacetanilide)-imino-diacetate into the circulating medium. DISIDA is only metabolized by active hepatocytes. After draining and flushing the circuit the cell aggregation foam was removed and cut into radial sections at the inlet, central and outlet portions along the bioreactor axis. These sections scanned for 10 minutes using a gamma camera. All values are presented as the mean $\pm$ standard deviation. Statistical significance was measured using Student's t test.

4.2.3 Results

Cell counts ranged between 6 x10^9 and 2 x10^{10} for all studies, with viability 95.91 % ±3.0%. Daily sampling: pO_2, pCO_2 and pH values averaged 286.5 ±25.5 mmHg, 30.0 ±1.4 mmHg and 7.45 ±0.03 respectively in both PFC(+) and PFC(-) cultures. Within the detection ability of the electrodes no significant drop in pO_2 was measurable when PFC was present. Thus, daily OUR determinations were only possible in PFC(-) cultures, average: 17.8 ±4.0 nmol/hr/10^6 cells. The gas carrying ability of PFC is far greater than that of MEM or plasma (figures 3.2.5,6). Since the majority of all other measurements of the PFC(-) and PFC(+) cultures were similar, OUR was assumed to be equivalent. Lactate values were similar in both cultures, while pyruvate values were slightly decreased in the PFC(+) cultures. Since an increase in the lactate to pyruvate ratio is generally due to an increase in anaerobic metabolism, it is possible that the difference may have been due to PFC interference in pyruvate measurement, rather than by an anaerobic state (although PFC was removed by centrifugation in all determinations). AST and LD concentrations decreased exponentially in the first 3 days of culturing, with initial levels of 217.9 ±60.7 IU/L and 98.4 ±50.8 IU/L respectively, descending to 23.0 ±19.5 IU/L and 48.2 ±22.4 IU/L by day 5. This would serve to indicate the progressive stabilization of the cell culture.

Metabolic clearance/production studies: D(+)galactose elimination on day 2 revealed that PFC(+) and PFC(-) cultures cleared similar amounts, 1.6 ±0.1 and 1.7 ±0.1 µg galactose/hr/10^6cells respectively. Monocultures cleared 0.35 ±0.2 µg/hr/10^6cells. Urea production on day 3 revealed that PFC(+) cultures produced 42.34 ±14.5 µg urea/hr/10^9cells, PFC(-) cultures produced 148.93 ±20.1 µg/hr/10^9cells and flasks produced 20.2 ±8.2 µg/hr/10^9cells. The differences in production may reflect interference with the measurement of urea in PFC(+) cultures. The clearance of ammonia was similar in the 3-D cultures; 8.2 ±3.0 µg ammonia/hr/10^9cells for PFC(+) and 8.6 ±4.4 µg/hr/10^9cells for PFC(-). The clearance of lidocaine on day 4 was 1.6 ±0.1 µg lidocaine/hr/10^6cells for PFC(-) cultures. PFC(+) cultures cleared lidocaine at 2.8 ±0.3 µg/hr/10^6cells which was significantly better than PFC(-) cultures ($p<0.05$). Monocultures cleared 0.6 ±0.4 µg/hr/10^6cells. The production of albumin on day 5 was similar in the 3-D cultures, PFC (-) cultures produced 21.9 ±0.9 µg albumin/hr/10^6cells, while PFC(+) cultures produced 21.9 ±0.5 µg/hr/10^6cells.

Upon termination on day 7, SEM confirmed the presence of hepatocyte aggregations in the open-cell matrix (figures 4.2.2,3). Isotopic imaging demonstrated that the distribution of actively functional hepatocytes in the matrix was determined by the flow of the circulating medium through the foam (figure 4.2.4). While there were irregularities in the foam it was taken that CFD had indeed been useful for bioreactor design.

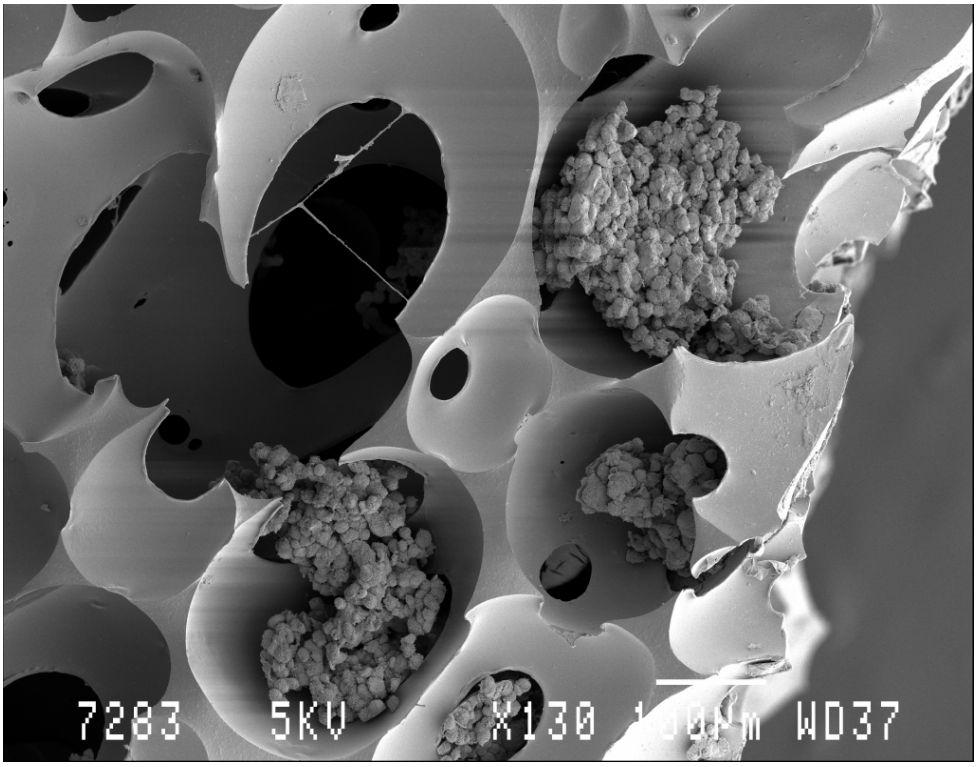

Figure 4.2.2 SEM image of open-cell PUF cell adhesion matrix with cell aggregations. Magnification: 250x.

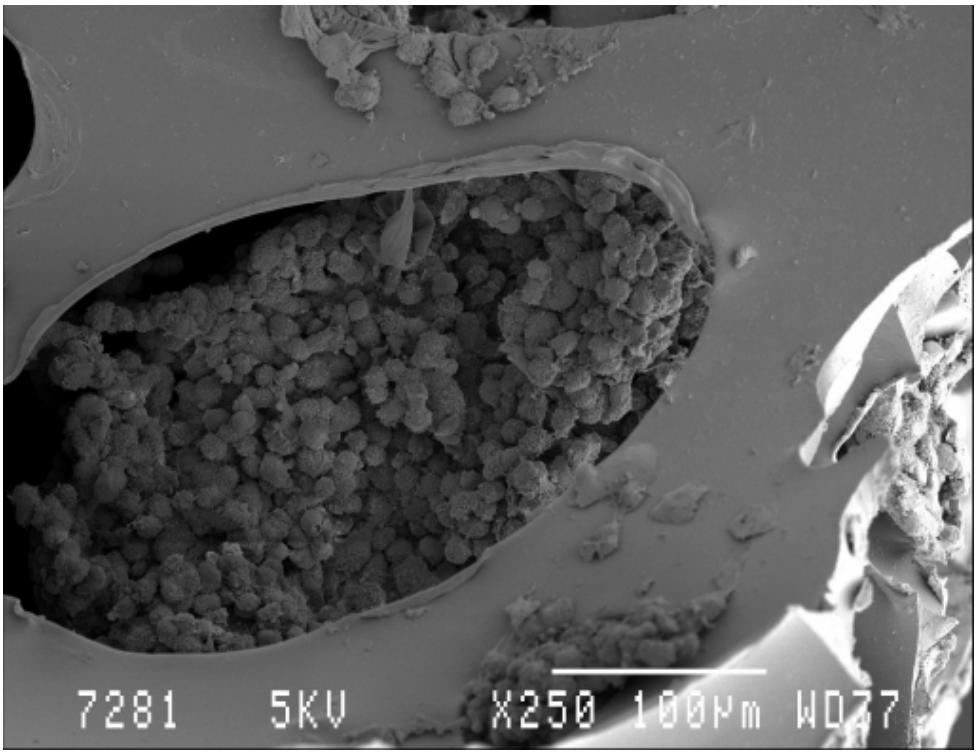

Figure 4.2.3 SEM Image of a single large cell aggregate in the PUF adhesion matrix. Magnification 130 x.

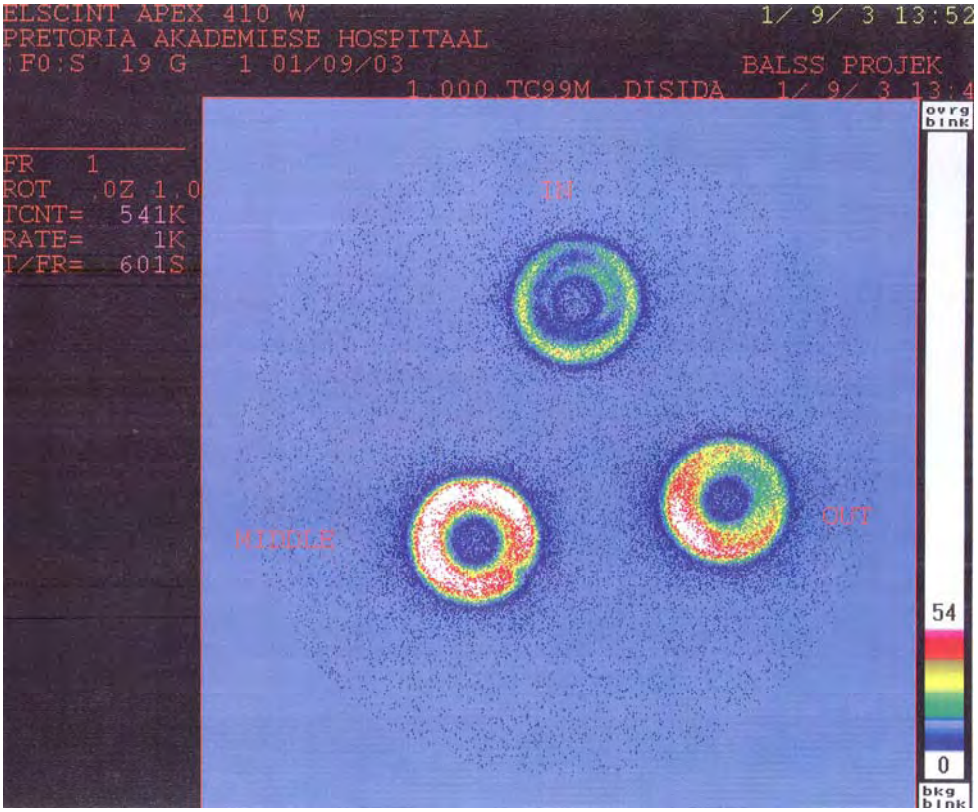

Figure 4.2.4 ^{99m}Tc-DISIDA isotope scan of PUF cell aggregation matrix. The radial-flow foam was sectioned into inlet, middle and outlet portions along the axis of the

bioreactor. White portions indicate large quantities of radio-labeled, actively functioning hepatocytes. Regions that appeared to be inhomogenously seeded were found to be due to irregularities (bubbles) in the foam and to inaccurately sliced sections. The cells aggregated according to the flow of the medium through the matrix.

4.2.4 Discussion

The interpretation and evaluation of the *in vitro* performance of an hepatocyte bioreactor is complicated by especially two factors: Firstly, to quote Hoekstra *et al* (2002) [125], "many researchers do not quantify BAL or cell functions as an absolute figure related to cell quantities functioning during a defined period", and secondly; when figures are available, very large divergences (in the values for various liver functions) are apparent (table 3.2.1). Whether this divergence is due to innate biological variation as a result of differences in the culture configuration, or due to differences in the analysis methods, remains to be answered. Until this is satisfactorily done, the complete confirmation of the metabolic efficacy of bioreactors for BALSS devices may remain impossible.

In this study observations suggested that the OUR of the UP-CSIR bioreactor tends to a limit determined by cell density and the pO_2 of the circulating medium. However, the usefulness of OUR as an indicator of the metabolic state of hepatocytes in a bioreactor is balanced by the challenge of its accurate determination in 3-D cultures. The assumption that the OUR measured for hepatocytes grown in monolayers is constant in 3-D culture configurations at high cell densities may be incorrect [98,107]. Previous investigations of the OUR of a variety of types of hepatocytes have revealed that as cell density and the pO_2 of a perfusing culture medium increases, OUR per unit cell mass decreases [126]. It has been proposed that the release of humoral factors controlling cell-cell communication may enable the cells to manage "crowding" by temporarily suppressing oxidative metabolism [127]. Perhaps the decrease in OUR with increasing cell density follows an allometric relationship such as that first described by Kleiber [128,129]? This relationship represents an evolutionary strategy whereby OUR is diminished with increasing body mass. There is utility in observing such a relationship: OUR may potentially be scaled to large cell numbers, enabling real-time functional quantification of a bioreactor.

Table 4.2.1 Variation in results for porcine hepatocytes

Author/s	Bioreactor Configuration	Clearance/ Production:	Reported as:	Converted to:
Flendrig *et al* [104]	Hollow-fiber with mesh	Urea	1.8±0.2 µg/hr/10^6 cells	1.8±0.2 µg/hr/10^6 cells
Abrahamse *etal* [105]	Hollow-fiber	Urea	5.5±0.4 µg/hr/10^9cells	$5.5x10^{-3}$±$4x10^{-4}$ µg/hr/10^6 cells
de Bartolo *et al* [100]	Flat membrane	Urea	25±5 ng/hr/cell	$25x10^3$±$5x10^3$ µg/hr/10^6 cells
Bader *et al* [101]	Flat membrane	Urea	80±10 pg/hr/cell	80±10 µg/hr/10^6 cells
Gerlach [106]	Multi axial hollow fiber	Urea	38.3 mg/hr/10^{10}cells	3.83 µg/hr/10^6 cells
Yanagi *et al* [103]	Microcarrier packed bed	Urea	$4.4x10^{-13}$±$1.5x10^{-13}$mol/hr/cell	26.4±9.0 µg/hr/10^6 cells
	Monoculture		$7x10^{-13}$±$2x10^{-13}$mol/hr/cell	42.0±13.8 µg/hr/10^6 cells
Nieuwoudt *et al*	**PUF matrix: -PFC**	**Urea**		**0.15±0.02 µg/hr/10^6 cells**
	+PFC			**0.04±0.01 µg/hr/10^6 cells**
	Monoculture			**0.02±0.01 µg/hr/10^6cells**
Abrahamse *etal* [105]	Hollow-fiber	Ammonia	25±10 µmol/hr/10^9cells	25±10 µmol/hr/10^9cells
de Bartolo *et al* [100]	Flat membrane	Ammonia	56±10 pg/hr/cell	$3.3x10^3$±$0.6x10^3$µmol/hr/10^9cells
Bader *et al* [101]	Flat membrane	Ammonia	14±0.5 pg/hr/cell	820±30 µmol/hr/10^9cells
Gerlach [106]	Multi axial hollow fiber	Ammonia	605 µmol/hr/10^{10}cells	60.5 µmol/hr/10^9cells
Nieuwoudt *et al*	**PUF matrix: -PFC**	**Ammonia**		**8.6±4.4 µmol/hr/10^9cells**
	+PFC			**8.2±3.0 µmol/hr/10^9cells**
Morsiani *et al* [102]	Radial flow mesh	Albumin	5.9±0.7 ng/24hr/10^6cells	$2.46x10^{-4}$±$2.92x10^{-5}$ µg/hr/10^6 cells
Gerlach [106]	Multi axial hollow fiber	Albumin	5.33 mg/hr/10^{10}cells	0.533 µg/hr/10^6 cells
de Bartolo *et al* [100]	Flat membrane	Albumin	1.4±0.2 pg/hr/cell	1.4±0.2 µg/hr/10^6 cells
Nieuwoudt *et al*	**PUF matrix: -PFC**	**Albumin**		**21.9±0.9 µg/hr/10^6 cells**
	+PFC			**21.0±0.5 µg/hr/10^6 cells**
Balis *et al* [130]	Monoculture	OUR	0.6±0.15 nmol/sec/10^6cells	$2.16x10^3$±$0.54x10^3$ nmol/hr/10^6cells
Morsiani *et al* [102]	Radial flow mesh	OUR	6±1 nmol/hr/10^6cells	6±1nmol/hr/10^6cells
Morsiani *et al* [102]	*Calculated from human liver	OUR	15 nmol/min/10^6cells	900 nmol/hr/10^6cells
Nieuwoudt *et al*	**PUF matrix: -PFC**	**OUR**		**17.8±4.7 nmol/hr/10^6cells**

Note: The above values are a selection of literature results and not intended as a summary or review. Certain values have been read off graphs and are thus approximate.* Value from *in vivo* human liver for comparative purposes.

In this study ammonia clearance, albumin production and galactose elimination were similar in the dynamic cultures and higher than in monocultures. Increased metabolic activity was therefore observed in dynamic compared to monolayer cultures. Urea production was increased in PFC(-) cultures relative to PFC(+) cultures, while lidocaine clearance was significantly higher in PFC(+) cultures. The increased lidocaine clearance in PFC(+) cultures may indicate that lidocaine metabolism (cytochrome P450) is more dependent on oxidative metabolism and higher O_2 tension than the other metabolic variables studied. Several previous investigators using PFCs in production bioreactors have noted significantly improved metabolic functions [131-133]. It was observed that similar results were obtained for PFC(+) and PFC(-) cultures for most variables studied. It should be borne in mind that there is 0.5 times more CO_2 and 4.5 times more O_2 present in a 20% v/v PFC emulsion relative to normal medium (figure 4.2.5). Thus, the benefit of adding PFC may only be apparent when high cell densities are employed in a bioreactor. If the O_2 carrying ability of plasma is taken to be approximately equal to that of medium it is clear that the emulsion would be far better at preventing hypoxia in high density, stressed cellular environments.

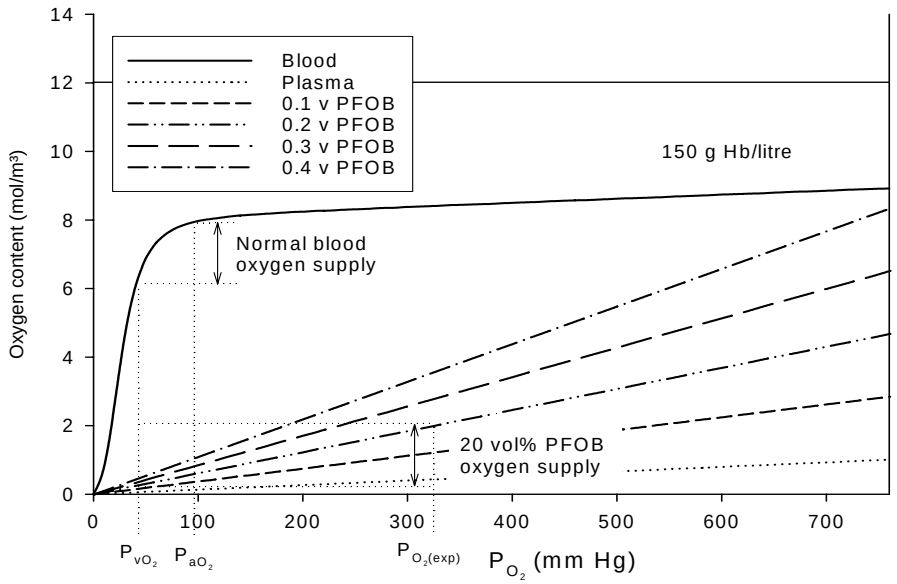

Figure 4.2.5 Increased PFOB volume fraction increases the oxygen carrying capacity of the emulsions. The oxygen solubility in the emulsions follows a linear relationship with partial oxygen pressure. The experimentally measured partial oxygen pressure in the UP-CSIR BALSS is indicated on the graph, showing similar potential oxygen delivery compared to blood (if exposed to normal venous partial oxygen pressure).

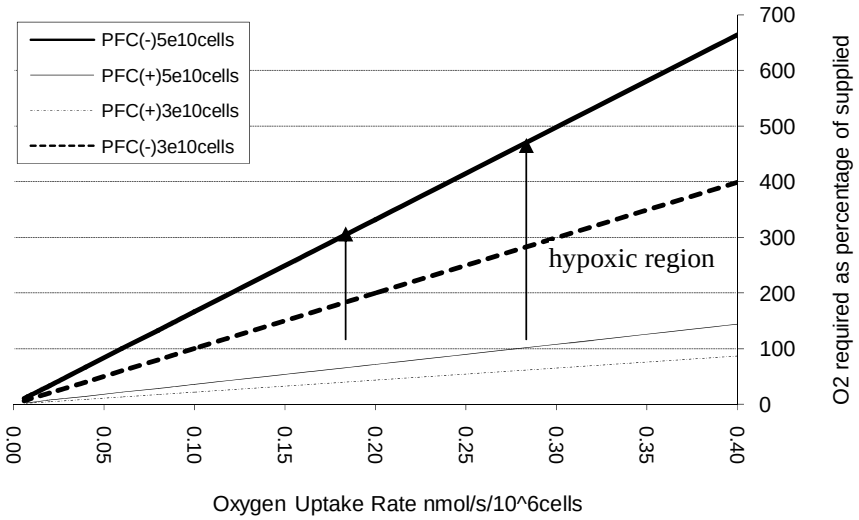

Figure 4.2.6 Simulation of bioreactor O_2 requirements. PFC emulsions provide a significant advantage to high cell densities in a BALSS. The cell densities in this study were insufficient to challenge the O_2 supplied to the bioreactor. The flow rate was 300 ml/min.

Additionally, calculations of bioreactor O_2 requirements, Moolman *et al* (2004) [10,94], indicated that with increasing OUR the demand relative to the supply of O_2 becomes severely limiting when PFC is not used (figure 4.2.6). It was also revealed that the present experiments were conducted at cell densities that were insufficient to challenge the O_2 supply of the bioreactor. This may explain why the metabolic performance was similar.

In conclusion, in this study it was observed that hepatocyte aggregation occurred in the PUF matrix of the bioreactor and metabolic functions were improved relative to flask cultures. The addition of PFC to the medium improved some hepatocyte functions such as lidocaine clearance and no adverse effects were otherwise detectable. Calculations indicated that the cell densities employed were insufficient to challenge the O_2 supplied to the bioreactor and this may explain the similarity in the results. The true benefits of PFCs are more likely to be found in preventing hypoxia when very high cell densities are employed in a bioreactor.

4.3 Imaging glucose metabolism in perfluorocarbon-perfused hepatocyte-stellate co-culture bioreactors using positron emission tomography

Nieuwoudt M, Wiggett S, Malfeld S, van der Merwe SW.

Journal of Artificial Organs, 2009;12:247-57.

4.3.1 Introduction

In vivo hepatic functional zonation, from periportal to perivenous along the sinusoid, is determined by gradients of oxygen (O_2), hormones, nutrients/metabolites, extracellular matrix components, and the non-parenchymal cell distribution [2,134]. This zonal heterogeneity includes energy, carbohydrate, lipid, nitrogen, bile and xenobiotic metabolism and enables the liver to function as a 'glucostat', i.e. to maintain stable blood glucose levels during feeding or fasting states [135-138]. The periportal zone functions optimally at blood pO_2 levels of 60-70 mmHg (13 % v/v), while the perivenous does so at 25-35 mmHg (4 % v/v) [2].

A variety of *in vitro* studies have shown that hepatocytes cultured in 2D and 3D configurations demonstrate metabolic functionality that is dependent on the pO_2 of the oxygenating gas mix [109,120,121,139-143]. In general, physiological O_2 gas mixes lead to gluconeogenesis, while hypoxic gas mixes lead to glycolysis. A glycolytic bioreactor metabolism is not ideal in that a similar pre-existing clinical condition may be exacerbated in treating an acute liver failure (ALF) patient. Maintaining a stable hepatocyte phenotype is also dependent on interactions with non-parenchymal cell populations, which constitute 30-35 % of the liver [86,134,144-147]. Recapturing hepatic functionality in bioreactors designed for bioartificial liver (BAL) devices requires particular attention to these facts.

Some BAL designs perfuse only plasma to avoid the coagulatory and immunological reactions associated with whole-blood exposure to extracorporeal materials. However,

under normal conditions approximately 98 % of the O_2 in whole-blood is carried by haemoglobin (Hb). Thus, atmospheric gas concentrations, metabolically active hepatocytes in plasma-only BALs are likely to become hypoxic and consequently exhibit glycolytic metabolism. Synthetic perfluorocarbons (PFC) are exceptionally inert and have excellent O_2 carrying properties. Their inclusion in the circulating medium or plasma therefore represents an attractive hemoglobin replacement solution without immunological consequences and may be used to emulate the heterogenous gas levels in the liver.

The O_2 carrying benefits of PFCs have been demonstrated in a limited number of *in vitro* studies, including 2D hepatocyte cultures [148-151] in alginate packed-bed 3D configurations and 3D microbial bioreactors [152-154]. However, in dynamically-circulating 3D primary hepatocyte or hepatocyte-stellate co-culture bioreactors this has not been conclusively shown to date. In a prior study we demonstrated that including a (20 % v/v) perfluorooctyl bromide (PFOB)-lecithin emulsion retained the metabolic functionality of hepatocyte bioreactors (section 4.2). Lidocaine clearance was significantly improved relative to PFC(-) controls but all other metabolite measurements were similar. Our calculations indicated that the O_2 level of the oxygenating gas mix (60 %) was likely too high to result in hypoxia in the PFC(-) bioreactors (section 4.2)[88].

A difficulty in demonstrating bioreactor metabolic functionality is limited access to the hepatocytes once they have aggregated in the matrix. Accessing them requires a bioreactor design that enables parts of the cell-containing matrix to be removed *during* operation without disrupting either the sterility or metabolic functionality of the system. Bioreactors are normally autoclaved for sterilization prior to application and subsequently remain sealed units. Flow cytometric or gene expression techniques that require the enzymatic liberation or lysis of cells from the matrix consequently result in the termination of an experiment. Similarly, there is also a lacking in consensus regarding the means of reporting metabolite production or clearance values and highly divergent results have been presented [125] (table 4.2.1 above). Thus, physiologically relevant, *in-situ* methods for demonstrating bioreactor metabolism remain desirable. Owing to its particular benefits, positron emission tomography (PET) may be one such method.

In this study, primary *in vitro* hepatocyte-stellate co-culture bioreactors with and without 20 % v/v perfluorooctyl bromide-lecithin emulsions were compared in terms of their O_2-dependent glucose uptake. The 20 % v/v level was selected based on optimal oxygenation and viscosity characteristics [10,94]. 'Hypoxic' and 'ambient' O_2 gas mixes were used as the oxygenating gas mixes. PET scans, using radioactive glucose (2-[^{18}F]fluoro-2-deoxy-*D*-glucose or ^{18}FDG) as the imaging label, were then conducted on the bioreactors within 24 hours following the primary cell isolation procedure [87], i.e. the same as would occur if a patient was to receive such a BAL treatment. PET is an attractive method for studying bioreactors in that it is well-established in the human clinical environment, provides metabolically relevant information and the results are visual and numerically quantifiable.

4.3.2 Materials and Methods

After gaining approval from the University of Pretoria Animal Use and Care Ethics committee, a total of 8 Landrace pigs were used in these experiments.

Media and chemicals

All media and chemicals used in the perfusion and transport of the livers are as described by Nieuwoudt *et al* (2005)[87]. Perfluorocarbon-lecithin emulsions were prepared according to the method of Moolman *et al* (2004)[10,94]. The emulsions were mixed with double concentrated cell culture medium and sterile deionised water, to achieve a 20 % v/v PFC emulsion-medium mixture. The mixture was adjusted to pH 7.35 – 7.4 and used as a culturing medium. In contrast to our earlier studies 'modified hepatocyte growth medium' (m-HGM)[155-159] was used for all cell culturing purposes. This formulation aimed to provide the best possible milieu for hepatocyte function. Please refer to Appendix A4 for the composition.

Cell isolation procedures

Hepatocyte isolation was performed according to the method of Nieuwoudt *et al* (2005) (section 4.1)[87]. After a clean hepatocyte-only suspension had been produced it was pumped out of the BRAT bowl through the emptying-line into an oxygenation

flask. The final volume of the suspension was noted for yield and viability calculations.

Simultaneous to the hepatocyte isolation procedure, stellate cells were fractionated from the non-parenchymal cell suspensions using the method of Riccalton-Banks *et al* (2003)[144]. Briefly, the cellular collagenase perfusate and discarded supernatant from the hepatocyte washings was pooled in a 1L Schott bottle and gently oxygenated. The cell suspension was poured into 50 ml centrifuge tubes then centrifuged for 5 mins at 50 g. The cell pellets were discarded after transferring the supernatant to new tubes and centrifuged again for 5 min at 50 g. The pellets were then discarded and the supernatant centrifuged for 10 min at 205 g. Thereafter, the supernatant was discarded and the pellet resuspended in 10 ml m-HGM. Two 10 min centrifuge (at 205 g) and pellet DMEM resuspension cycles followed. The remaining cells were confirmed to be stellates using microscopy.

Bioreactor seeding and evaluation methods

After evaluating the cell suspensions from the above procedures for viability and cell count the suspensions (hepatocytes and stellates) were pooled into one container and divided in half to make two volumes of 300 ml m-HGM with an equal number of cells in each. These volumes were transferred to the bioreactor reservoirs and re-circulated into two identical 150 ml radial-flow bioreactors to allow ‘seeding’ in the open-cell polyurethane foam (PUF) cell-aggregation matrices as previously described [79]. The medium was circulated at 50 ml/min in the two identical sterile, sealed circulation systems and driven by a single peristaltic pump. This system represented a two bioreactor *in vitro* dynamic model of the BAL device and was housed in a non-gas non-humidified incubator at 37.5 ^{o}C (figure 4.3.1 below). The medium in the reservoirs was oxygenated using an autoclavable aquarium bubbler using a single high pO_2 gas mix source (60% O_2, 5% CO_2, balance N_2) which facilitated hepatocyte aggregation/seeding in the PUF matrix. Previous studies have demonstrated that high pO_2 levels facilitate hepatocyte aggregation following cell isolation procedures [120,121,126,139].

After 4 hours of circulation and seeding, the medium containing the remaining non-aggregated cells was discarded and replaced with fresh medium. One bioreactor was given normal m-HGM while the other received the PFC-m-HGM mixture as described above. The oxygenating gas was then changed to 'hypoxic' (5% O_2, 5% CO_2, balance N_2) or 'ambient' (20% O_2, 5% CO_2, balance N_2) mixes depending on the experiment in progress. The term 'ambient' was used in view of the similarity of the particular O_2 level to that of air (21 %). These gas mixes were selected based on calculations by ourselves (section 4.2), and the findings of prior studies [109,120,121,139]. They were chosen to discriminate differences in O_2-dependent carbohydrate metabolism, i.e. glucose uptake between PFC(+) and PFC(-) cell-seeded bioreactors.

Steady-state medium sampling

After 24 hours of oxygenation and circulation, sterile 1 ml media samples were taken from the sampling ports of both bioreactors for the electrochemical detection of steady-state pH and gas partial pressures, pO_2 and pCO_2. A Chiron diagnostics Rapidlab 865 clinical blood gas analyzer (Bayer, South Africa) was used for this purpose. At the same time, media samples were also taken in duplicate and immediately frozen for glucose, lactate and pyruvate detections to investigate bioreactor carbohydrate metabolism as represented by the composition of the circulating extra-cellular medium. Standard spectrophotometric laboratory kits were used for this purpose (Sigma-Aldrich kits 472500 for glucose, 445875 for lactate and 726 for pyruvate).

Figure 4.3.1 The dual bioreactor *in vitro* model/s of the BALSS. The PFC reservoir and bioreactor are on the left (pink). The PFC(-) medium reservoir and bioreactor are on the right (red). Compare this configuration with the earlier single version (figure 4.2.1 above).

Bioreactor transport and PET imaging

The bioreactors were then removed from the incubator and transported to the Little Company of Mary hospital PET facility in Pretoria, South Africa. Recirculation was maintained throughout by powering the peristaltic pump with a 12 volt car battery and a 220 volt inverter. The media in the reservoirs was also oxygenated using the particular gas mix being tested in each experiment. The duration of transport was no more than 20 minutes, allowing minimal loss of bioreactor temperature.

At the PET facility the bioreactors were placed on the scanning bed of a Siemens Biograph 6 CT-PET machine and then centralized with respect to the gantry. Media recirculation and oxygenation was continued throughout. The standard brain scan image data acquisition program was loaded.

Independent 2.1 ± 0.01 mCi IV-syringe doses of ^{18}FDG were eluted from the on-site Eclipse RD cyclotron and associated Explora FDG_4 automated chemical synthesis unit. In these instruments deoxyglucose is labeled with ^{18}F ($t_{1/2}$ = 110 min) by nucleophilic displacement of an acetylated sugar derivative (1,3,4,6-tetra-*O*-acetyl-2-*O*-trifluoromethane-sulfonyl-β-*D*-mannopyranose) followed by hydrolysis with hydrochloric acid. The hyrolysate then passes through a C-18 Sep-Pak column and yields ^{18}F-2-fluoro-2-deoxyglucose (^{18}FDG).

Each bioreactor was sequentially subjected to an identical procedure. The ^{18}FDG dose was injected into the respective PFC(+) or PFC(-) bioreactor circuit's sampling port and circulated in the medium for 15 minutes allowing uptake by the resident cells. Thereafter, the radioactive medium was discarded followed by 2 x 5 minute washout cycles using 150 ml of fresh non-radioactive medium after which that was also discarded. This ensured, firstly, that any radioactivity remaining in a given bioreactor accounted for only glucose taken up by cells, and secondly, that a minimal amount of the PFC remained in the cell aggregation matrix. Each bioreactor was scanned with the brain scan program for 20 minutes, first by computed tomography (CT) for positioning, followed by PET for ^{18}FDG absorption. Image slice intervals were set to 4 mm. Since positron-electron extinction reactions result in coincident gamma photons, the selective detection of these photons by the PET machine results in inherently 3-dimensional images.

Image analysis and reporting

CT-corrected PET images were reconstructed using the system's Syngo (Siemens) image processing software. This fuses the anatomical (CT) data with the functional (PET) data and enables the rotation of the reconstructed bioreactor in 3-D. The resulting files were then transferred to a Siemens multimodality workstation (MI applications 2006A). A volume of interest was drawn around *only* the cell aggregation matrix within each bioreactor in 3 axes i.e. the transverse, sagittal and coronal. The ^{18}FDG radioactive 'heat' or count density (in Bq/ml) for the volume of interest was then recorded. Reports were drawn up by slicing each bioreactor through its midline in the above axes and displayed in rows from the top down of the PET images, then the CT images, then the fused CT-PET images (figures 4.3.2,3). The report for each

bioreactor was printed using a HP colour laser printer. 3D-rotatable video reconstructions were also generated and saved to CD-rom.

Following PET scanning the bioreactors were returned to the laboratory and dismantled. The PUF foam from each bioreactor was removed and photographed to confirm that cells were present.

Statistics and calculations

Microsoft Excel (2003) was used as the spreadsheet for all data. Mean and standard deviations were calculated where possible. Statistix 8, (Analytical software, Tallahassee FL, USA) was used when significant differences ($p<0.05$) were calculated with two-sample T tests.

The dissolved gas concentrations in the recirculating medium were calculated using the method of Moolman *et al* (2004)[10,94]. i.e. these were either [theoretical]'s calculated from absolute atmospheric levels compared to [measured]'s calculated from the electrochemical results:

$$C_{CO_2/O_2,total} = \left[\frac{\emptyset_p}{H_{CO_2/O_2-p}} + \frac{1-\emptyset_p}{H_{CO_2/O_2-w}}\right].P_{CO_2/O_2-w}$$

$in\ \frac{mol}{m^3}\ and\ pressure\ in\ bar$

where,

$\emptyset_p = PFOB\ volume\ fraction\ in\ emulsion,$

$P_{CO_2/O_2-w} = partial\ gas\ tension\ for\ CO_2\ or\ O_2$ in acqueous/water/plasma phases, in bar

$H_{CO_2/O_2-p} = Henry's\ constant\ for\ CO_2\ or\ O_2\ in\ PFOB\ at\ 37^oC$

$H_{CO_2/O_2-w} = Henry's\ constant\ for\ CO_2\ or\ O_2\ in\ water\ at\ 37^oC$

with constants:

$H_{O_2-p} = 0.0516\ bar.\frac{m^3}{mol}$

$H_{O_2-w} = 0.95\ bar.\frac{m^3}{mol}\ in\ water$ or $0.988\ bar.\frac{m^3}{mol}\ in\ blood\ plasma$ (taken as ~ equivalent)

$H_{CO_2-p} = 0.0121\ bar.\frac{m^3}{mol}$

$H_{CO_2-w} = 0.0394\ bar.\frac{m^3}{mol}\ in\ blood\ plasma$

and assumptions:

1. The gases were completely equilibrated in all phases, e.g. $pO_{2\ (water)} = pO_{2\ (gas)}$. This is reasonable in that the 0.2 µm droplets have a large surface area for mass transfer and measurements were taken following 24 hours of in-gassing.
2. The medium was maximally gas loaded, ie. pCO_2 and pO_2 were at their maximum when the CO_2 in the gas mix was 5 %.
3. O_2 consumption and CO_2 release by cells was not taken into account in that the medium was in-gassed maximally during the experiments.

4.3.3 Results

Since the BRAT centrifuge bowls used for isolating hepatocytes were all of a fixed volume (165 ml) and the stellate isolation procedures were identical, the total cell quantities remained approximately equivalent, i.e. a mean of 1.852×10^{10} hepatocytes and 1.84×10^8 stellates prior to sub-division for the two bioreactors. The number of PET experiments conducted per experimental group, the mean number of cells seeded per bioreactor (9.26×10^9 hepatocytes and 1.84×10^8 stellates), the calculated gas concentrations, the electrochemically measured media pH and gas partial pressures 24 hours after isolation and the mean radioactive glucose uptake per bioreactor are presented in table 4.3.1. Figures 4.3.2 and 4.3.3 are PFC(-) and PFC(+) bioreactor CT-PET scans respectively.

A total of 16 PET scans were conducted: Four pairs on cell-seeded bioreactors using the ‘hypoxic’ (5 % O_2) gas mix, two pairs on cell-seeded bioreactors using the ‘ambient’ (20 % O_2) gas mix and two control pairs on cell-free bioreactors using each of the above mixes. In all the hypoxic and ambient scans, cell–seeded PFC(-) bioreactors were more radio-active than PFC(+) ones. This was significant in the ‘hypoxic’ experiments, i.e 57 % ($p = 0.01$), not so in the ‘ambient’ i.e. 62 % ($p = 0.3$), but significantly so when they were combined, i.e. a mean of 59.5 % ($p = 0.04$). Thus, more glucose was taken up from the circulating medium by cell-seeded PFC(-) bioreactors than PFC(+) ones, indicating a more glycolytic metabolism in the former. Since the ‘ambient’ PFC(-) experiments were more radio-active than their PFC(+)

counterparts, it suggested that the 20 % O_2 gas mix may also have been slightly *hypoxic* for the cells.

As expected, the cell-free controls scans were similar, although both demonstrated that PFC(-) bioreactors were more radio-active than PFC(+) bioreactors: 23.7 % and 15.4 % respectively, i.e. a mean of 19.6 %, combined p = 0.5. Glucose absorption by binding to the *non*-reactive PFC emulsion may be excluded in that the levels of circulating extracellular glucose in the cell-free PFC(-) and PFC(+) configurations were similar. Thus, the most probable cause of the difference was Compton photonic scattering by the high atomic mass PFC molecules remaining in the cell-aggregation matrix, i.e. the long carbon and fluorine 'backbone' of the PFOB ($C_8F_{17}Br$) and any remaining lecithin protein. Despite the initial PFC concentration of only 20 % v/v and the thorough PFC-free medium washout and discardation cycles, it was apparently not possible to eliminate all of the PFC in the matrix. However, equal initial amounts of PFC were used in all bioreactors. Thus, it was possible to exclude the scattering effect by *normalizing* with the difference between the controls, i.e. by subtracting the mean % difference between the cell-free bioreactors, 19.6 %, from the mean % difference between the cell-seeded bioreactors. This resulted in differences of 36.4 % and 42.4 % for 'hypoxic' and 'ambient' PFC(-) versus PFC(+) configurations respectively. Clearly, PFC(-) cell-seeded configurations remained more glycolytic than their PFC(+) counterparts. Visual examination of the individual scans (figures 4.3.2,3) and the 3D video reconstructions also confirmed this difference in each case.

Table 4.3.1 Seeded cell counts, PET-bioreactor radiation counts (^{18}FDG-uptake) and electrochemical pH and gas results, 24 hours after cell isolation procedures

group	gas mix	[theoretical]	cells/ bioreactor	PET counts/bioreactor	measured media pH and gas partial pressures		[measured]
hypoxic (N=4)	5%O_2, 5%CO_2, balance N_2	PFC(-) O_2 = 0.05 PFC(+) O_2 = 0.24 PFC(-) CO_2 = 1.27 PFC(+) CO_2 = 1.84 **PFC(-) O_2/CO_2 = 0.04** **PFC(+) O_2/CO_2 = 0.13**	9.26x10^9 hepatocytes 1.84x10^8 stellates	PFC(+): 3.29x10^4±2.28x10^3 PFC(-): 7.94 x10^4±1.89 x10^4 **(-) > (+): 57.0 + 9.99 %**	PFC(+) pH: 7.615 ±0.021 pO_2: 108.03 ±5.53 pCO_2: 13.48 ±5.51 **pO_2/pCO_2: 8.02**	PFC(-) pH: 7.664 ±0.299 pO_2: 71.74 ±0.79 pCO_2: 24.603 ±0.32 **pO_2/pCO_2: 2.92**	PFC(-) O_2 = 0.10 PFC(+) O_2 = 0.55 PFC(-) CO_2 = 0.83 PFC(+) CO_2 = 0.86 **PFC(-) O_2/CO_2 = 0.12** **PFC(+) O_2/CO_2 = 0.97**
hypoxic control (N=1)	5%O_2, 5%CO_2, balance N_2	as above	0	PFC(+):1.77 x10^4 PFC(-): 2.32 x10^4 **(-) > (+): 23.7 %**	PFC(+) pH: 7.61 pO_2: 67.8 pCO_2: 21.4 **pO_2/pCO_2: 3.17**	PFC(-) pH: 7.46 pO_2: 67.2 pCO_2: 24.0 **pO_2/pCO_2: 2.80**	
ambient (N=2)	20%O_2, 5%CO_2, balance N_2	PFC(-) O_2 = 0.21 PFC(+) O_2 = 0.94 PFC(-) CO_2 = 1.27 PFC(+) CO_2 = 1.84 **PFC(-) O_2/CO_2 = 0.16** **PFC(+) O_2/CO_2 = 0.51**	9.26x10^9 hepatocytes 1.84x10^9 stellates	PFC(+): 2.05x10^4±1.28x10^4 PFC(-): 5.24x10^4±2.81x10^4 **(-) > (+): 62.0 ± 4.0 %**	PFC(+) pH: 7.797 ±0.117 pO_2: 113.6 ±12.45 pCO_2: 9.72 ±1.67 **pO_2/pCO_2: 11.69**	PFC(-) pH: 7.449 ±0.023 pO_2: 106.96 ±12.67 pCO_2: 22.42 ±1.67 **pO_2/pCO_2: 4.77**	PFC(-) O_2 = 0.15 PFC(+) O_2 = 0.73 PFC(-) CO_2 = 0.79 PFC(+) CO_2 = 0.77 **PFC(-) O_2/CO_2 = 0.19** **PFC(+) O_2/CO_2 = 0.95**
ambient control (N=1)	20%O_2, 5%CO_2, balance N_2	as above	0	PFC(+): 4.65x10^4 PFC(-): 5.49x10^4 **(-) > (+): 15.4 %**	PFC(+) pH: 7.61 pO_2: 117.3 pCO_2: 21.4 **pO_2/pCO_2: 5.48**	PFC(-) pH: 7.445 pO_2: 116.0 pCO_2: 24.1 **pO_2/pCO_2: 4.81**	
prior studies	60%O_2 90%O_2	PFC(-) O_2 = 0.63 PFC(+) O_2 = 2.83 PFC(-) O_2 = 0.96 PFC(+) O_2 = 4.29					

Footnotes:

1. All values given as mean ± std dev.
2. Units of ^{18}FDG radiation count density in bioreactor matrices is in Bq/ml
3. Units of measured pO_2 and pCO_2 is mmHg.
4. [ ] = gas concentration in mol/m^3
5. [theoretical] and [measured] was calculated as per the method of Moolman *et al.* [10,94]. See Methods for details.
6. The mean difference in the PET counts for the cell-free controls: PFC(-) vs. PFC(+) was 19.6 %.
7. There was a significant difference between the FDG radioactivity counts of hypoxic cell-seeded PFC(-) vs. PFC(+) bioreactors (57 %, p = 0.01). Not so in the ambient cell-seeded bioreactors (62 %, p = 0.3), but significant when combined (59.5 %, p = 0.04).

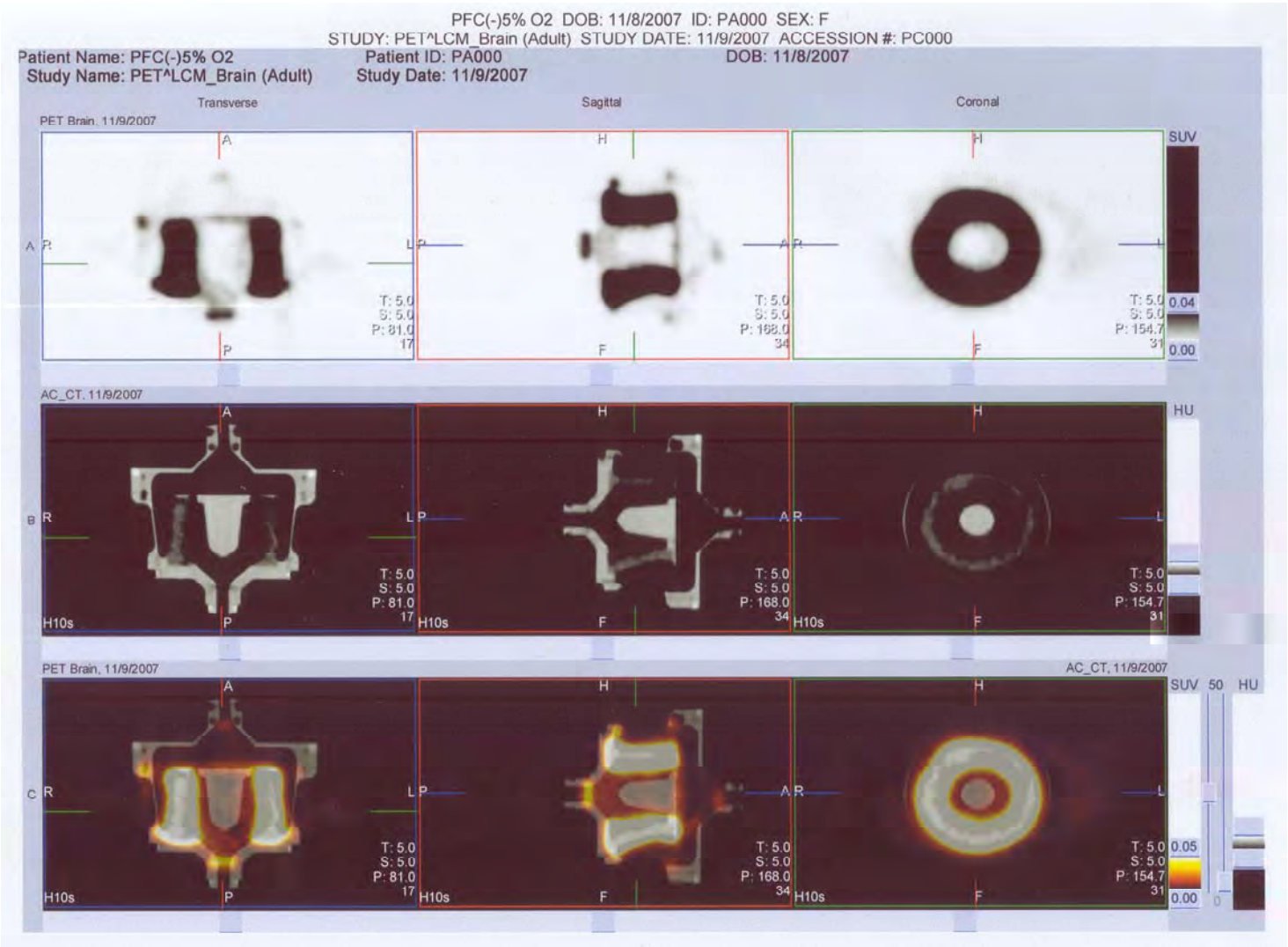

Figure 4.3.2 CT and PET scan of hypoxic gas mix cell-seeded bioreactor *without* PFC. The first row of images are PET only, the second CT only, the third is the combined CT (in black and white) and PET (in colour) images. The columns represent the transverse, sagittal and coronal planes respectively. The PET images of PFC(-) bioreactors were more radioactive or 'hotter', following greater glucose uptake, i.e. with a more glycolytic metabolism than the PFC(+) bioreactors.

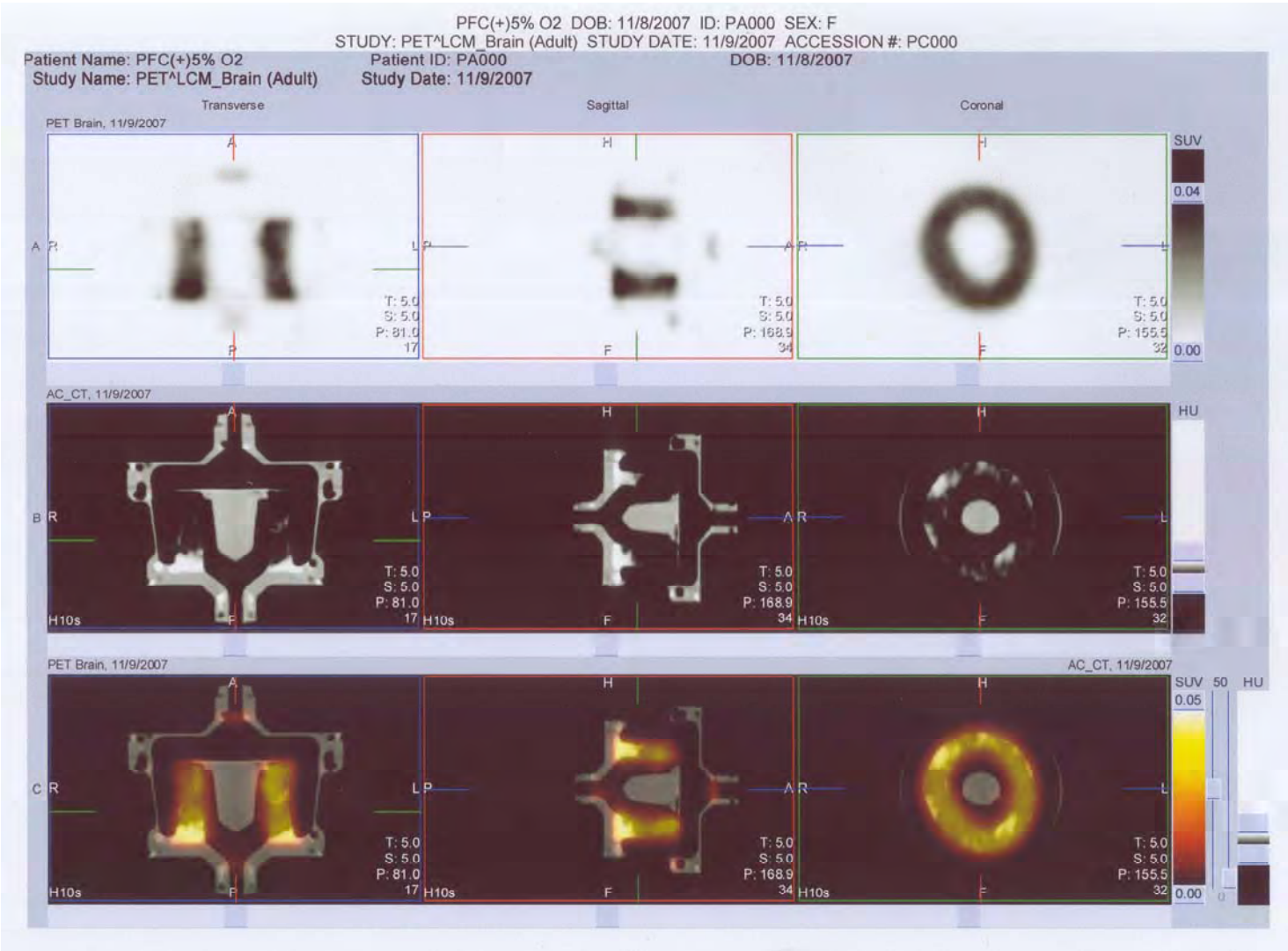

Figure 4.3.3 CT and PET scan of hypoxic gas mix cell-seeded bioreactor *with* PFC. PFC(+) bioreactors were all 'cooler' having absorbed less glucose, i.e. less a glycolytic metabolism than PFC(-) bioreactors.

The metabolic 'steady state' biochemistry (table 4.3.2), as represented by the composition of the extracellular medium 24 hours after isolation demonstrated in both hypoxic and ambient situations that glucose levels were higher and lactate levels were lower in cell-seeded PFC(+) versus PFC(-) bioreactors. This was significant for glucose in the hypoxic situation ($p < 0.01$) but not so in the ambient ($p = 0.5$). No other significant differences were detectable, although measurement variation and the small sample sizes must be considered. These results were in agreement with the PET results in that the PFC(-) bioreactors were more glycolytic than the PFC(+) ones. Interestingly, pyruvate levels were higher in the PFC(-) cell-seeded circumstances, which was unexpected from a glycolytic versus gluconeogenic perspective. From these and prior experiments (section 4.2) it would suggest that either the phospholipidic lecithin PFC emulsifier or the PFC itself interfered with the pyruvate detection method.

Table 4.3.2 Steady state biochemistry at 24 hours post isolation

Group		glucose	lactate	pyruvate
hypoxic	PFC(+):	28.08 ±2.94	2.60 ±0.16	58.63 ±16.98
	PFC(-):	26.44 ±0.73	2.71 ±0.14	89.25 ±27.99
Hcontrol	PFC(+):	33.13 ±0.96	2.21 ±0.36	70.00 ±11.83
	PFC(-):	27.20 ±0.14	1.64 ±0.14	65.50 +16.26
normoxic	PFC(+):	23.58 ±1.76	2.33 ±0.14	39.25 ±7.63
	PFC(-):	22.26 ±1.87	2.40 ±0.28	126.0 ±47.29
Ncontrol	PFC(+):	25.10 ±5.00	2.20 ±0.87	97.50 ±4.04
	PFC(-):	25.68 ±1.22	2.28 ±0.67	100.0 +10.39

Footnotes:

1. There was a significant difference between the glucose levels of hypoxic cell-seeded PFC(-) vs. PFC(+) bioreactors ($p < 0.1$), but not so in the ambient levels ($p = 0.5$). No other significant differences were detectable.
2. Units of glucose and lactate are in mmol/l, pyruvate in µmol/l

The absolute gas concentrations in the medium that were calculated from atmospheric pressures, i.e. the [theoretical]'s, demonstrated greater O_2/CO_2 ratios in PFC(+) versus PFC(-) bioreactors in both hypoxic and ambient circumstances (table 4.3.1). There is little doubt that these differences would have impacted O_2–dependent metabolism in the bioreactors. In the electrochemically measured results, greater pO_2/pCO_2 ratios were apparent in all PFC(+) cases, more so when there were cells than not. However, we have repeatedly found that Clarke–type electrodes, as are found in blood gas machines, produce highly divergent measurements for dissolved O_2 or CO_2 in PFC emulsions. This was visible in the difference between the [theoretical]'s and that calculated from

the measured (pCO_2, pO_2) results, i.e. the [measured]'s and the apparent alkalosis, associated with low pCO_2 levels, in the PFC(+) circumstances. However, in all ratios for PFC(+) experiments a trend was visible. The raised (calculated and measured) O_2/CO_2 and pO_2/pCO_2 values relative to the PFC(-) experiments suggested that O_2 provision to the cells had been improved by PFC in all cases.

4.3.4 Discussion

Several techniques have historically been employed to overcome O_2 limitations in hepatocyte cultures and bioreactors, including for example, optimizing the porosity of the extra cellular matrix (ECM) [160], the incorporation of perfluorocarbon-based O_2 carriers in the ECM [161], the use of bovine hemoglobin O_2 carriers in the circulating medium [162] and increasing the number and diameter of gas carrying hollow fibres (HF) in bioreactors [163]. A simplistic approach is to increase the pO_2 of the oxygenating gas mix. However, this is potentially hazardous in that large hepatocyte aggregates may be exposed to hyperoxic conditions externally, while remaining hypoxic in their internal regions and resulting in an increase in cell mortality [161]. Including a 20 % v/v PFOB-lecithin emulsion in the circulating medium is a feasible method, without immunological impacts, for replacing circulating hemoglobin and attaining a milieu similar to the metabolic zonation found in the *in vivo* liver.

The gas mixes used in this study to represent either hypoxic or ambient/normal situations were based on prior examples [109,120,121,139] and calculated estimates by ourselves (section 4.2). However, some uncertainty remained since bioreactor oxygenation characteristics vary according to design and are therefore different in each case. The bioreactors used in this study were an improved form of an earlier version [79] (figures 3.1,2 and 4.2.1). Extensive flow optimization, mass transport improvement and the minimization of dead-space had subsequently occurred [112]. Thus, flow dynamics in this case would obviously differ from that in 2D culture flasks or 3D HF-bioreactors. Our results suggest that the ambient (20 % O_2) gas mix may also have been slightly hypoxic to the cells. This was despite findings to the contrary in a previous 2D *in vitro* study employing the same gas mix [120].

Mareels *et al* (2006) [163], found by numerical modeling and experimentation that a large majority of the cells in an earlier iteration of the AMC hollow-fiber bioreactor were hypoxic using a 60 % O_2 gas mix. As a result, the AMC bioreactor's internal configuration and oxygenating gas was altered to a 95 % O_2 mix. We have reservations regarding this approach. Our results suggest an ideal O_2 level > 20 %, but certainly < 60 % as was previously employed by us. Additional numerical modeling and experimentation will aid in resolving this figure in the future.

In agreement with a prior study [164], we have found that electrochemical methods, e.g. blood gas machines, are not ideal for measuring the O_2 dissolved in PFC emulsions. This was evident in the difference between the [theoretical]'s calculated from atmospheric pressure and the [measured]'s calculated from the electrochemical results. The measured pO_2 and pCO_2 values (table 4.3.1) represent that in predominantly the aqueous phase and do not accurately account for the substantially more gas dissolved in the micellar-organic phase. Unfortunately, aqueous pO_2 and pCO_2 levels can only indirectly be compared with that measured in whole blood or the organic phase of PFC. However, our results did indicate improved theoretical O_2/CO_2 and measured $pO2/pCO_2$ ratios associated with PFC in all cases. This would suggest that PFC had improved the delivery of O_2 to cells in all cases.

Clinical imaging technologies have previously been employed in studying hepatocyte bioreactors. This has been done using magnetic resonance imaging (MRI), [112,165-169], once by ourselves using single photon emission tomography (SPET) with ^{99m}Tc-DISIDA (figure 4.2.4 above), but apparently never with PET. Two studies used PET to image bioartificial myocardial grafts in a solid matrix [170,171] and one for a tissue engineered trachea [172]. In general, MRI provides anatomical and/or flow information, while SPET and PET provide physiological information. In ^{18}FDG-PET the oxygen in glucose is replaced with Fluorine-18 and owing to its short half life ($t_{1/2}$ = 110 mins) *non-invasive in vivo* studies of carbohydrate metabolism are possible [173]. PET scan data is inherently 3-dimensional owing to the electronic scintillation detection of 180-degree coincident photons originating in a positron-electron extinction reaction. The resolution of the images is high owing to the coincidence detection methodology. PET scans of *in situ* hepatocytes in bioreactors require the latter to be constructed of materials that are sterilizable and radio-transparent to 511 keV gamma photons. In this

case the bioreactors were machined out of polycarbonate, which is autoclavable at 121 ^{o}C and provides no obstruction to such photons.

All the PET scans in this study indicated more glycolytic metabolism in cell-seeded bioreactors without PFC.The extracellular 'steady state' glucose and lactate levels were in agreement with this but also with another study using a similar rationale and which investigated the incorporation of PFC into the ECM [162]. Taken together, this may be accepted as confirmation of the success of our procedures. Bearing in mind the normal clinical purpose of ^{18}FDG-PET, namely to examine glycolytic lesions such as cancer in human patients, [173], it is perhaps unsurprising that it was successful in this case. Having said that, maintaining *exactly* the same experimental conditions was necessary throughout and success must partly be owing to this.

Since the application of PET in this case was novel it was necessary to estimate the radioactive doses. In view of the necessity of discarding the washout media, to maximally control the experimental conditions and decrease radiation exposure to personnel, and the fact that the employed bioreactors were sealed units following their autoclaving prior to cell-seeding, it was not possible to gather information using methods that would require cell liberation or lysis from the cell aggregation matrix. This study was 'short term', i.e. on the same time-scale following cell isolation as would occur in BAL treatments using primary cells. However, hepatocyte metabolism is diverse and may change with the duration of culturing. In the future, the use of lower ^{18}FDG doses may allow longer term, e.g. 5-10 day bioreactor investigations *after* PET scans. It will then be interesting to additionally investigate the effect of improved O_2 provision by PFC on nitrogenous and/or xenobiotic hepatocyte metabolism. No studies thus far have investigated the effects of PFC on bioreactor longevity.

In conclusion, this study demonstrated that ^{18}FDG-PET was an effective imaging modality for investigating the *in-situ* O_2-dependent metabolism of hepatocyte bioreactors in conditions simulating those likely to be found in plasma-only BAL treatments. Agreement for the PET results was found in the circulating extracellular metabolites. In the future longer term metabolic studies will provide complimentary information to the above.

4.4 Thoughts and recommendations

The above *in vitro* cell biology and bioreactor studies presented a large scale, sterile primary cell isolation procedure, an investigation of hepatocyte metabolism over 7-days in a direct plasma-contact hepatocyte bioreactor and the novel use of PET to discriminate between O_2 challenged PFC versus non-PFC flow optimized bioreactors.

From a simple statistical perspective the primary cell isolation method has been very successful: In 40 procedures over a 3 year period, a mean of $2.14 \times 10^{10} \pm 8.60 \times 10^{8}$ hepatocytes and $2.43 \times 10^{9} \pm 1.82 \times 10^{8}$ stellate cells were isolated from the livers of 30 kg pigs with liver masses of approximately 1.5 kg each. Bacterial or fungal contaminations were not found in any of these, which verified the sterility of the procedures.

Of interest, assuming an adult liver has between 1.0 and 1.5×10^{11} hepatocytes, 2.14×10^{10} equates to approximately 15 – 20 % of the total amount, or assuming the liver is composed of 70 % hepatocytes and has a mass of 1.5 kg, the isolated hepatocyte mass weighs 158 – 210 g. These values are within the amount often quoted to be sufficient for an effective bioartificial liver support device [70,83,92]. Having said that, it is ideal to have as large a cell mass as possible, assuming the conditions in the bioreactor are sufficient to maintain them. The disposable BRAT bowls used in the above method were of a fixed volume (either 250 or 165 ml) which limited the total amount of cells that could be isolated. There are consequently efforts underway to use other larger volume apparatus which will increase the isolatable quantity.

The second study successfully demonstrated that there was metabolic activity in both PFC and non-PFC bioreactors over a 7 day period, but presumably due to the employed gas mix was unable to show a difference between them. During the course of this study and in unpublished efforts subsequently, some of the difficulties involved in successfully demonstrating the efficacy of such bioreactors was further highlighted. For example, the mentioned lack of consensus regarding reporting methods, the great variations in reported results and the difficulty of measuring *in situ* cell functions due to a lack of non invasive methods enabling direct access to them. In specifically the latter,

we found that the PFC and fragments of the PUF matrix were difficult to remove from cell aggregate samples taken from dismantled bioreactors after termination. Gene expression and flow cytometry experiments were consequently unreliable.

The subsequent novel use of PET was an attempt to solve the above problems and to conclusively demonstrate that the PFC facilitated cell function under hypoxic conditions, as may be found in the treatment of an acute liver failure patient. They were also performed on the same duration following a primary cell isolation procedure that would occur if such cells were employed in the BAL device. The success of the experiments was partly owing to the use of radio-transparent bioreactor material and attention to maintaining exactly the same experimental conditions.

4.4.1 Developments in cell sources

The obstacle which is arguably solely responsible for preventing the entrance of bioartificial liver technology into the commercial arena is the establishment of a renewable source of sterile, metabolically effective, immunologically safe and affordable cells in sufficient quantities.

Primary human hepatocytes are the obvious ideal choice owing to minimal immunological concerns. However, their low availability and the difficulty of maintaining metabolically effective cells in *in vitro* cultures have prevented their widespread use [174]. Primary porcine hepatocytes are an attractive alternative owing to their easy availability, low cost and their maintenance of metabolic functionality in culture. Ongoing concerns regarding xenozoonoses have prevented their use. European law forbids the use of xenogenic tissue in any human treatments [70].

4.4.1.1 Genetically engineered swine

Despite EU law, no porcine endogenous retrovirus (PERV types A,B and C) infection has been recorded in *in vivo* human cells, neither has any disease resulting from this family of viruses been found in either humans or pigs [175,176]. PERVs also appear to be susceptible to currently available antiviral therapies [177,178]. Thus, assuming the immunological differences between pigs and humans are overcome and animals are

raised in *guaranteed* pathogen-free conditions, the attractiveness of porcine tissues as a cell or organ source remains.

There have been significant advances in genetic engineering: α-1,3 galactosyltransferase gene-knockout (GT-KO) pigs have been developed that no longer express the Galα1,3Gal(Gal) oligosachiride and thus avoid responses from the natural antibodies for this in humans [179]. The PERV infectivity of porcine tissue has been inhibited by the introduction of an RNA interference silences gene (siRNA) [180]. Several of the coagulation-anticoagulation incompatibilities between humans and pigs have also been recognized [181]. Animals transgenic for human anticoagulation genes, such as CD39 [182], tissue factor pathway inhibitor [183] and human complement regulatory proteins (CRP) such as CD46 and CD55 are currently being developed [184,185]. Several other genes such as TFPI, DAF, CD59, HLA-E, ULBP-1 and CD47, are also believed to be important [176]. Thus, while the ideal would be a pig transgenic for all of the above, it does not yet exist. Judging by the pace of progress in this field (and there being no associated physiological complications) it seems reasonable to expect such an animal within the next 10-15 years.

The above developments are indeed auspicious in terms of the establishment of a cell source for a BAL device. However, the focus of the above research has been to develop an animal appropriate for xenotransplantation rather than for simply a hepatocyte source. Assuming success, the fact that the only therapy of proven survival benefit for ALF is OLT, the need for developing an extracorporeal BAL device may be negated. Naturally, unforeseeable developments in the future preclude drawing this conclusion at this time it simply remains an interesting possibility.

4.4.1.2 Chimeric animals

The *in vitro* propagation of human hepatocytes is difficult. For this reason researchers have begun engrafting and expanding human hepatocytes in animals. Two systems are being studied: Urokinase-type plasminogen activator-transgenic severe combined immunodeficiency mice express uroplasminogen activator (uPA/SKID mice) under the transcriptional control of a hepatotoxic albumin promoter. These immunodeficient knockout mice do not reject infused human hepatocytes. As the murine hepatocytes die

they are replaced with unaffected human cells, yielding chimeric human/mouse livers with engraftment levels up to 92 % [186]. Drawbacks to this system include difficulties in animal husbandry, predisposition to renal disease in the immunodeficient animals and difficulties in controlling the mutant hepatocyte phenotype enabling only a narrow time window for engraftment [187,188].

An alternate system developed in response to the above is as follows: Immunodeficient fumarylacetoacetate hydrolase gene/recombination activation gene/interleukin-2 receptor gamma gene ($Fah^{-/-}/Rag^{2-/-}/Il2rg^{-/-}$) 'triple knockout' mice develop an essential hepatocyte deficit due to tyrosemia induced by the omission of the fumarylacetoacetate hydrolase gene. Following pre-treatment with a urokinase expressing adenovirus these animals allow human cell engraftment from many sources including liver biopsies. Serial hepatectomy with human hepatocyte repopulation has been possible up to four times and the expanded cells demonstrate typical human drug metabolism. These animals are easy to breed, do not develop renal disease and are transplantable several times [188,189].

The above *in vivo* systems are still in early development and only limited testing of the metabolic functionality of the mutant cells has occurred. Assuming these approaches are found reliable, the system may be adapted to a large animal such as the (ever reliable) pig to overcome the limitation in expanded cell numbers present in the murine model [174]. From hepatectomized animals such as the latter, a large scale sterile hepatocyte isolation procedure as presented above can then be performed.

4.4.1.3 Concerns regarding other cell types

Stem, tumorigenic and transformed cell types replicate extensively in *in vitro* culture. However, growing sufficient cells in a sterile manner is a significantly more costly undertaking than isolating primary cells. For example, assuming one needs to generate a quantity of 400 g of cells to seed into 1 or 2 bioreactors for a single BAL treatment. (This amount equates to approximately 40 % of the hepatocyte mass of an innate liver):

Table 4.4.1 Simple accounting of expense differences (in South African Rand) between primary and transformed cells for a quantity of 400 g of hepatocytes

Item (primary)	Quantity	Expense	Item (transformed)	Quantity	Expense
Animal (pig)	2	3000			
Surgery + husbandry	2	6000			
Perfusion fluids	2	1600			
Isolation media (collagenase + density gradient)	2	3000	Cell liberation enzyme (trypsin)	10 x100 ml	2000
BRAT disposables	2	1800			
Centrifuge tubes	100	4000	Cell culture flasks	400 x 75cm^2	12000
Media	10 L	800	Media	60 L	24000
Salary (2 people)	1 day	2500	Salary (1 person)	1.5 months	30000
TOTAL		**22700**			**68000**
DIFFERENCE					**factor 3**

Note: These costs exclude research into developing the cell type (e.g. a transgenic animal or a transformed embryonic stem cell) and the overhead laboratory costs.

The difference in the two cell sources amounts to a 3-fold increase in costs associated with the 2-D culturing of the transformed cell type. Additionally, there are significant implications in terms of the time it takes to generate these quantities. Assuming the consistent clinical availability of BAL bioreactors, a GMP-certified laboratory must be growing the requisite large quantities of the cells *in parallel and at all times* [communication with Mr Greg Dane, ex-CEO of the US company Circe]. The cost differences then escalate a factor of 6 to 9 times that of a primary cell source.

Transformed cells are also potentially problematic in view of 'metabolic inappropriateness', in ALF. The question is, since their genotype and/or phenotype is different to a mature primary hepatocyte, are their expressed metabolic paths synthesizing or transforming metabolites in the same way as a healthy liver? For example,

The immortalized human hepatoblastoma C3A cell line, derived from a parental HepG2 lineage, has extensively been grown *in vitro* and clinically employed in the ELAD hollow fibre bioreactor [74]. However, despite reported improvements in HE, these cells synthesize urea by non-urea cycle (arginase II dependent) pathways and therefore do not detoxify ammonia [190]. HepG2 and possibly also C3A cells incorporate ammonia into glutamine via glutamine synthetase [191]. Although glutamine is not inherently toxic to the brain, this strategy is of questionable safety due to its astrocytic build-up in HE. The above underlies the multi-systemic syndrome of ALF (and HE),

but in addition to concerns regarding tumorigenicity, the non-ideal metabolic properties of this particular cell type are indicated. It therefore seems surprising that the US company Vital Therapies using ELAD (http://www.vitaltherpies.com), were successful in Beijing and consequently granted FDA approval to proceed with the ongoing Phase II trial in the US.

A large variety of stem cells are being researched as cell sources for BAL devices, but difficulties with the control of proliferation and differentiation to a mature phenotype remain [69,192]. Unfortunately, proliferation and differentiation in hepatocytes are usually diametrically opposed [82]. For example, cBAL111, a human telomerase reverse transcriptase (hTERT) immortalized human fetal hepatocyte cell line with a good proliferative capacity was recently developed [193,194]. However, this cell has a limited capacity for ammonia detoxification through urea production or to perform cytochrome P450 detoxification. Glycolytic lactate production in the bioreactor may also exacerbate this condition in a patient. Whether the immortalizing gene can truly be turned-off has also not been confirmed. Thus, while efforts at developing cell lines are justified (indeed important), the associated difficulties have prevented their wide acceptance to date.

Hepalife, a US based company, have found in *in vitro* trials that their patented PICM-19 pig epiblast cells [195,196] are able to retain ammonia detoxification, urea synthesis and cytochrome P450 functions at near porcine primary hepatocyte levels for an extended period (14 days) when exposed to human plasma [197]. The bioreactor employed in their system is that originally developed by Gerlach *et al* [198]. Hepalife has also recently purchased the patents, FDA approved IND and intellectual property of the company Arbios which owned the HepatAssist technology [199]. Historically, HepatAssist arguably progressed the furthest, in phase II/III BAL human trials, on the path towards device commercialisation [75]. HepaLife intends conducting large animal trials in the near future. However, despite all of these promising indications, the immunological considerations in employing cells of porcine origin remain.